2008

Trajectory and spray control planning on unknown 3D surfaces for industrial spray painting robot

Fanqi Meng
Iowa State University

Trajectory and spray control planning on unknown 3D surfaces for industrial spray painting robot

by

Fanqi Meng

A thesis submitted to the graduate faculty

in partial fulfillment of the requirements for the degree of

MASTER OF SCIENCE

Major: Industrial Engineering

Program of Study Committee:
Frank Peters, Co-Major Professor
Matthew Frank, Co-Major Professor
Huaiqing Wu

Iowa State University

Ames, Iowa

2008

TABLE OF CONTENTS

LIST OF TABLES

LIST OF FIGURES

ABSTRACT

Automated 3D path and spray control planning of industrial painting robots for unknown target surfaces is desired to meet demands on the production system. In this thesis, an image acquisition and laser range scanning based method has been developed. The system utilizes the XY projection of the boundaries of the target surface to generate the gun trajectory's X and Y coordinates as well as the spray control. Z coordinates and gun direction, distance, and speed are generated based on the point cloud from the target that is acquired by the laser scanner. A simulation methodology was also developed which is capable of calculating the paint thickness across the target surface. Results have shown that the generated path could perform a full coverage on the target surface, while keeping the paint material waste at the minimum. Excellent paint thickness control could be achieved on 2D and straight line sweep surfaces, while a satisfactory thickness is obtained on other 3D arbitrary surfaces. Relationships among thickness, spray deposition profile, sampling roughness and geometric features of the target surfaces have been discussed to make this method more applicable in industry.

CHAPTER 1 INTRODUCTION

Spray painting provides products or parts with an attractive appearance and protection against the environment. Automated spray painting has been extensively studied and practiced due to its advantages of low labor cost, high productivity and high consistency of surface finish quality. Most of the previous research has been focused on the automated painting of components of known shape and orientation, and the methods are either by manually teaching on the actual target surface, or based on the CAD model of the object. However, in today's trend toward a highly modularized and customized production line, it is more desirable to have the methods that could be adapted to the automated painting on unknown surfaces.

The problem of automated spray painting on unknown 3D arbitrary surface is solved by the following general steps in this thesis. The first step is X-Y motion planning and spray control planning based on a 2D projected image. Next, the Z coordinates of the center of the spray cone, the spray gun's direction, distance (See Figure 1-1.) and motion speed are all calculated base on 3D surface scanning. Finally, 3D path trimming based on the result of 2D spray control planning is determined. The whole system is described in Figure 1-2.

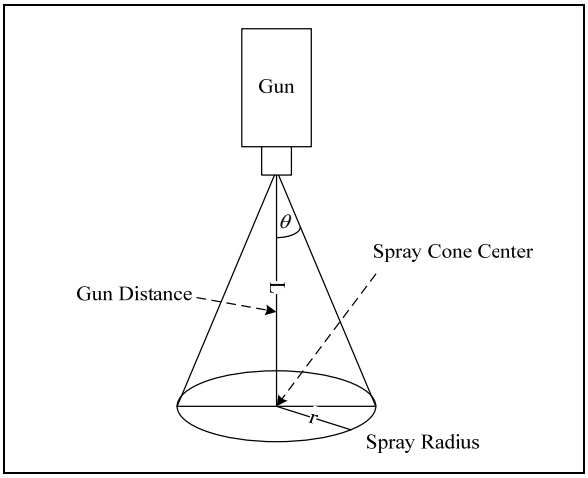

Figure 1 - 1 Spray Painting Model

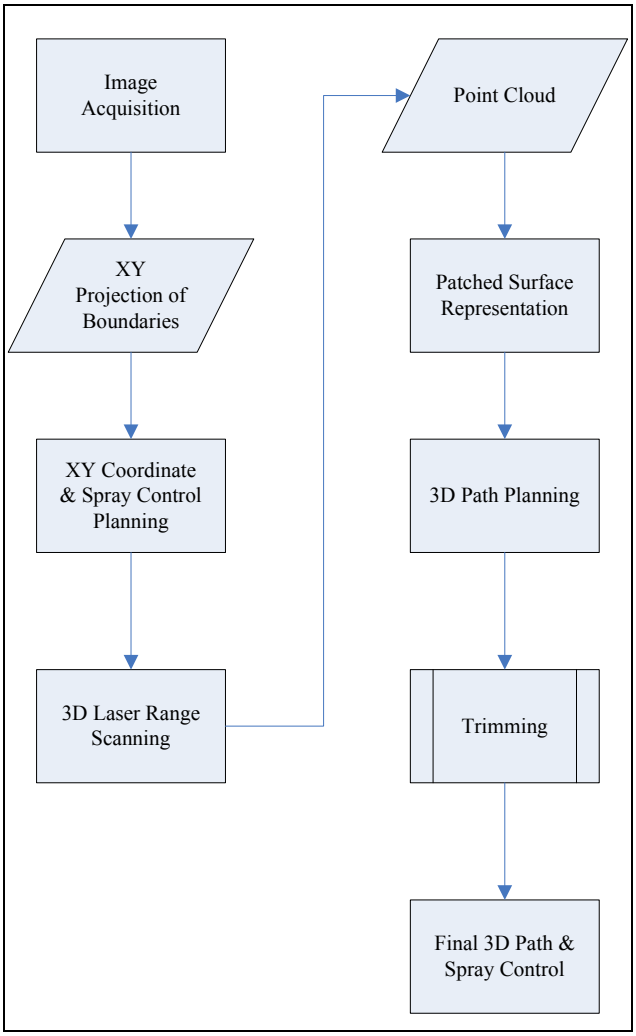

Figure 1 - 2 Flowchart of 3D Path Generation System

In most of the previous work on automated spray painting path generation, the target surfaces are assumed to have an ideal boundary without sharp corners or holes [1-10]. However, this is impractical in practice, especially when the target surfaces are unknown. Multi-scanning line and interval union methods are developed in this work to guarantee full coverage and to keep the waste of painting material at the minimum. Uniformity is controlled through the local 3D coordinate relationship analysis and varying the gun distance and motion speed accordingly.

In addition to the theoretical algorithm, the path planning results are implemented by a software program written in LabVIEW. This method has been shown to be adaptive to irregular outside-boundary 3D freeform surfaces with holes. Simulation results shows that the methodology presented in this paper could provide a full coverage on the

arbitrary 3D surfaces. Minimal variation of paint thickness could be achieved for 2D and straight line sweep surfaces, and for the 3D freeform surfaces, thickness variation could be controlled within a satisfied range.

CHAPTER 2 LITERATURE REVIEW

A spray painting model was established in the work of Suh et al. [1] and Arikan [2], where mathematical relationships between the painting thickness and other painting process parameters were analyzed. CAD model based 3D surface painting problem was widely investigated [3-5]. Sheng et al. [3] first introduced the pre-partition of the surface model according to local curvatures, and determined the painting parameters according to the thickness constrains. Chen et al. [4, 5] further analyzed the mathematical relationship between the trajectory model of the gun and the spray painting profile model, and determined the selection of painting parameters to achieve an optimized thickness. The similar goal was achieved by Prasad et al. [7] through a "seeded curve" selection, and then repetitively optimizing the painting gun speed and index width. Comparing with the automated spray painting based on CAD model, research that is adaptive to unknown surfaces is quite less. Anand et al. [9] developed an on-line robotic spray painting system using machine vision. However, the ability of the system is very limited as it could only recognize 2D objects and perform path planning. Laser range scanner was applied in the work of Pichler et al. [10] to detect the features of the target surface and match with the models in the pre-established library, but this method is error-prone considering the dimensional variability of the products, the orientation deviations during the scanning and the limitation of the model storage in the library.

CHAPTER 3 METHOD

3.1 Image Acquisition and Processing

Before entering the painting booth, parts will go through the image acquisition process, to have the boundaries and holes identified. With the parallel light source as the background, the body of the part could be captured by the camera and identified as the polygons filled by black pixels. Connecting the pixels on the edge of the black polygons will give the boundaries of the image. Ideally, the target surface of a part should be oriented perpendicular to the light beams, in order to have the shape captured accurately. However, due to the nature of an arbitrary3D surface, it is almost impossible to reach that ideal situation. Thus, keeping it as perpendicular as possible will minimize the error.

The boundaries of a surface image need to be further processed in order to be utilized by the following steps. To identify the location of the surface boundaries, they will have to be assigned with directions. By the “left hand rule”, when following along a boundary, the material should always fall on the left hand side, so for an outside boundary, it is counterclockwise, and for a inside boundary, it is clockwise.

3.2 Image Based Spray Control Planning

In order for the system to be adaptive to paint on surfaces with holes or vacant regions, an ON/OFF control of the spray is developed by using a ‘status combined multiple search lines’ algorithm, which is described below. Search lines are virtual horizontal lines that are used to intersect with the boundaries.

3.2.1 Single search line intersects single section of a boundary

For this algorithm, a control point here is defined as the intersection of a search line with a section of the boundary loop. A section is a connection of two neighboring points along a boundary. As illustrated in Figure 3-1, the coordinate of the control point A is given by:

$$Y = Yc$$

$$X = X_1 + (X_1 - X_2) \times (Yc - Y_1)/(Y_1 - Y_2),$$

with constraints:

$$Min(X_1, X_2) \le X \le Max(X_1, X_2),$$

where $(X_1, Y_1), (X_2, Y_2)$ are consecutive points along the direction of a boundary loop.

A special case is that if the section of a boundary is horizontal, such as the BC section in Figure 3-1, then the number of intersections will be infinite. In such case, no control point will be determined.

Spray control status at an intersection depends on the values of Y_1 and Y_2:

Spray is ON if $Y_1 > Y_2$; OFF if $Y_1 < Y_2$

3.2.2 Single search line intersects multiple sections of a boundary

Following the method described in the above section, the intersections and the corresponding spray status could be determined for a single search line intersecting with multiple sections of a boundary loop.

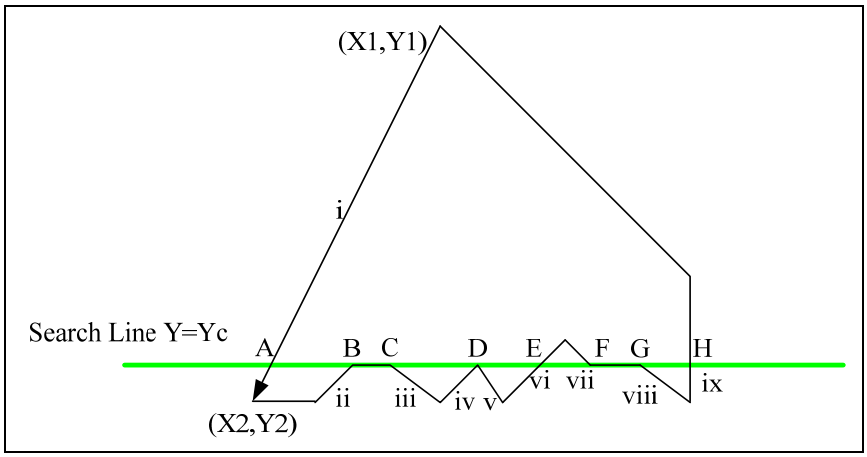

Figure 3 - 1 Determination of Control Points by a Single Search Line

For example, in Figure 3-1, the control points determined by the search line are shown in Table 3-1

Table 3 - 1 Initial Determination of Control Points

A	B	C	D	D	E	F	G	H
i	ii	iii	iv	v	vi	vii	viii	ix
ON	OFF	ON	OFF	ON	OFF	ON	ON	OFF

The first row of Table 3-1 lists the indices of the control points; the second row

lists the indices of the sections on the boundary loop; the third row gives the corresponding status of the spray. There is redundancy of the intersection and control status in the table, which will be reduced according to the following Reduction Rules.

Reduction Rule 1 *(Reduction of duplicated control points):*

When more than one spray status is determined at a single control point: if the status is the same, only one copy of them should be kept; if the status differs, the intersection is a dilemma point, and should be dropped.

Reduction Rule 2 *(Reduction of duplicated status for neighboring control points):*

For the same status on neighboring control points, the point with minimum X coordinate is most powerful and should be kept.

Table 3-3 and 3-4 show the results after Reduction Rule 1 and 2, respectively.

Table 3 - 2 Result after Reduction Rule 1

A	B	C	E	F	G	H
ON	OFF	ON	OFF	ON	ON	OFF

Table 3 - 3 Result after Reduction Rule 2

A	B	C	E	F	H
ON	OFF	ON	OFF	ON	OFF

3.2.3 Single search line intersects multiple boundaries

After the reductions, the result will be clear for the single search line intersecting a single boundary loop. For the XY projection of a real surface, there is no overlapping for any two boundary loops. Thus by combining the results of the each single loop, and sorting according to the X coordinates in ascending order, the result for a single search line intersecting with multiple boundary loops could be obtained.

3.2.4 Selection of search lines in a single spray stroke

Dynamically, spray painting is realized by generating a series of spray spots that cover a region along the trajectory of the spray gun, which is also called stroke. Assuming that the direction of the motion is along the X axis, to control the ON/OFF of the spray, it is necessary to combine all the control points' information along the search lines that are packaged within the stripe of the spray's projection on the XY Plane. Ideally, the number

of packed scanning lines should be infinite to gain a perfect result – a full coverage. However, computing an infinite number of scanning lines is infeasible, and even finding a great number of finite intersections also consumes a significant amount computer time. Fortunately, the following method could help determine the number and the locations of scanning lines, and still guarantees full coverage of the spray on the target surfaces.

Within a horizontal stripe of the spray, to guarantee the full coverage, search lines are determined by:

Selection Rule 1

Horizontal lines crossing the upper and lower bounds of the spray stripe should be included.

Selection Rule 2

The horizontal lines crossing the vertices of the target surface's boundary, which are within the upper and lower bounds of the spray stripe model should also be included (See Figure 3-2).

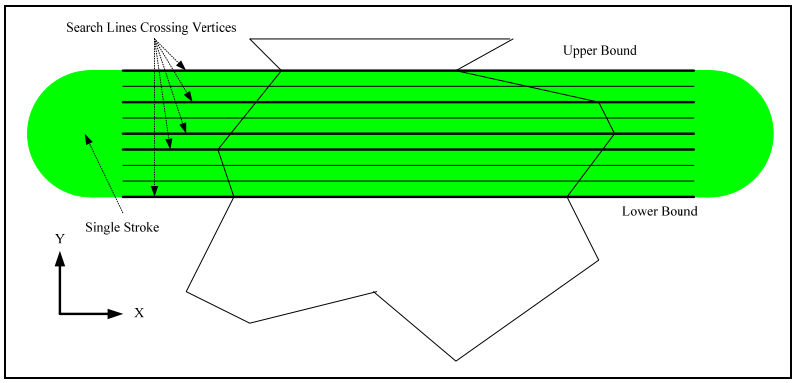

Figure 3 - 2 Selection of Search Lines within a Stroke

Selection Rule 3

Depending on the maximum allowable lost of coverage in the Y dimension, equally spaced horizontal lines should also be included. In practice, a spacing value of 0.1 inch would be enough. This rule works together with Reduction Rule 1 to make the system capable to work at the "sharp corner start" and "sharp corner stop" situations. As illustrated in Figure 3-3, Search Line Y1 is determined by Selection Rule 2, which crosses the vertex A. Since section CA is pointing downward, control point A should be

determined as ON. However, section AD is pointing upward, control point A now is determined as OFF. Thus by Reduction Rule 1, control point A is a dilemma point, which should be eliminated. With the help of Selection Rule 3, Search Line Y2 is determined, which will generate control points C-ON, and D-OFF. In this way, spray could be controlled to start at a sharp corner. Similarly, Selection Rule 3 determined Search Line Y3 to turn the spray off at the sharp corner EBF.

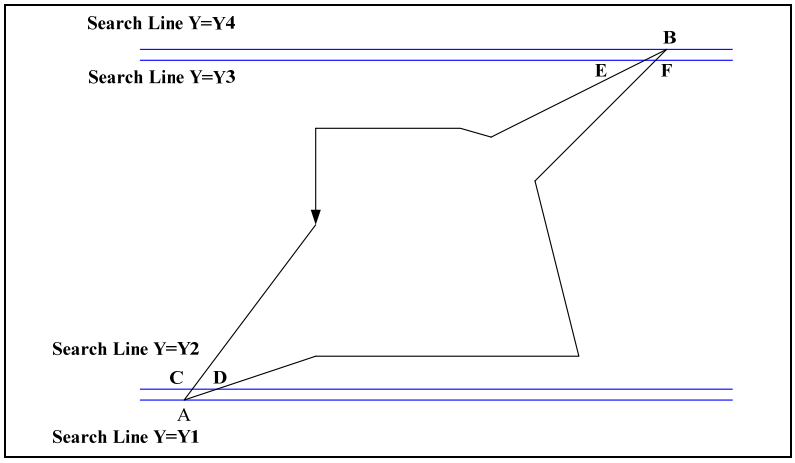

Figure 3 - 3 Sharp Corner Start and Stop

3.2.5 Control of spray within a single stroke

This subsection describes the method for integrating the control information of individual search lines to generate the ON/OFF spray control of a single gun stroke. In order to have a full coverage, any two of control point pairs (each ON-OFF is defined as a control pair) with overlap of X coordinates should be combined according to the following rule:

Combination Rule

The spray should be turned on at the smaller X coordinate of the control point with an ON status, and be turned off at the larger X coordinate of the control point with an OFF status within the two control pairs.

This rule should be executed for all the control pairs until there is no overlapping in X coordinates among the remaining control pairs. The detailed steps are described in the flowcharts in Figure 3-4 and Figure 3-5.

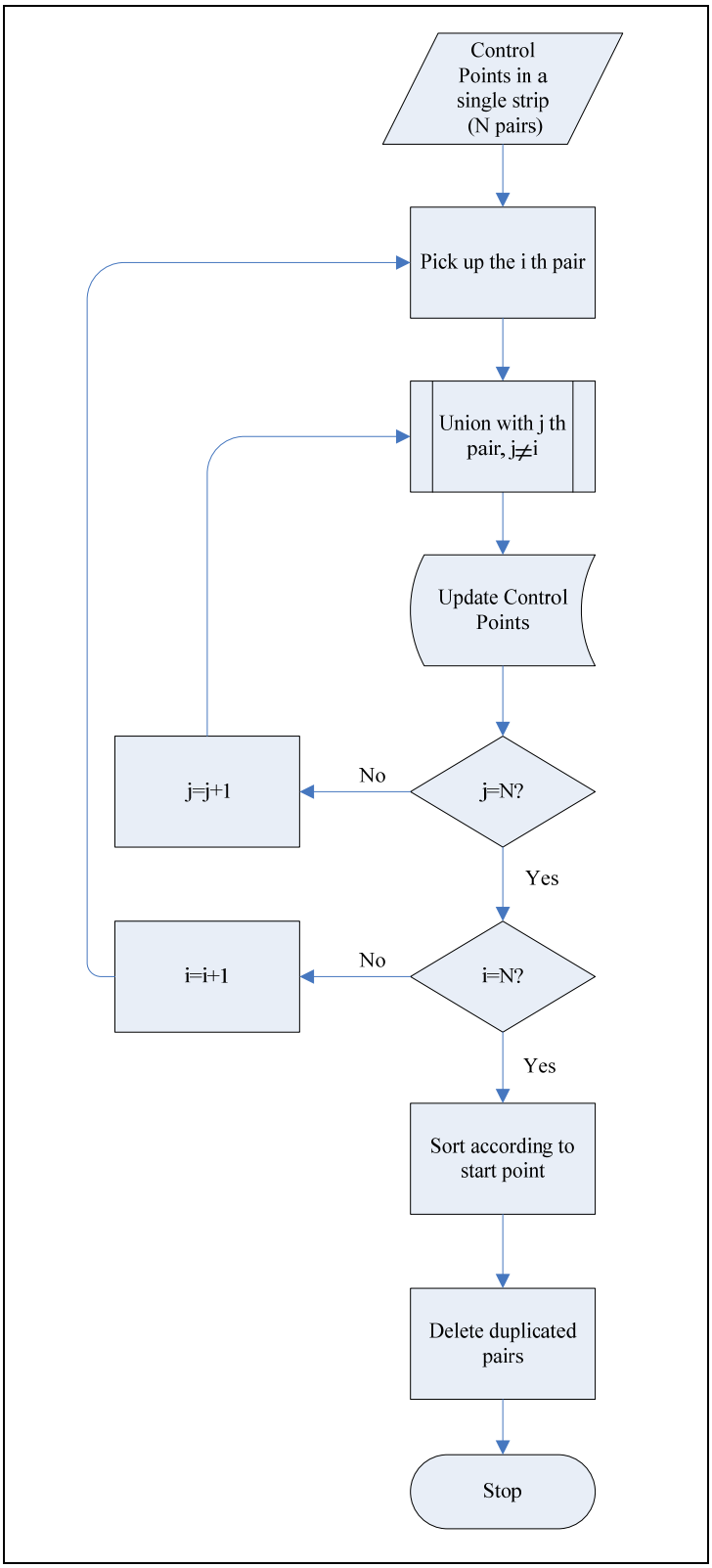

Figure 3 - 4 Flowchart of Generation of Spray Control in a Single Gun Stroke

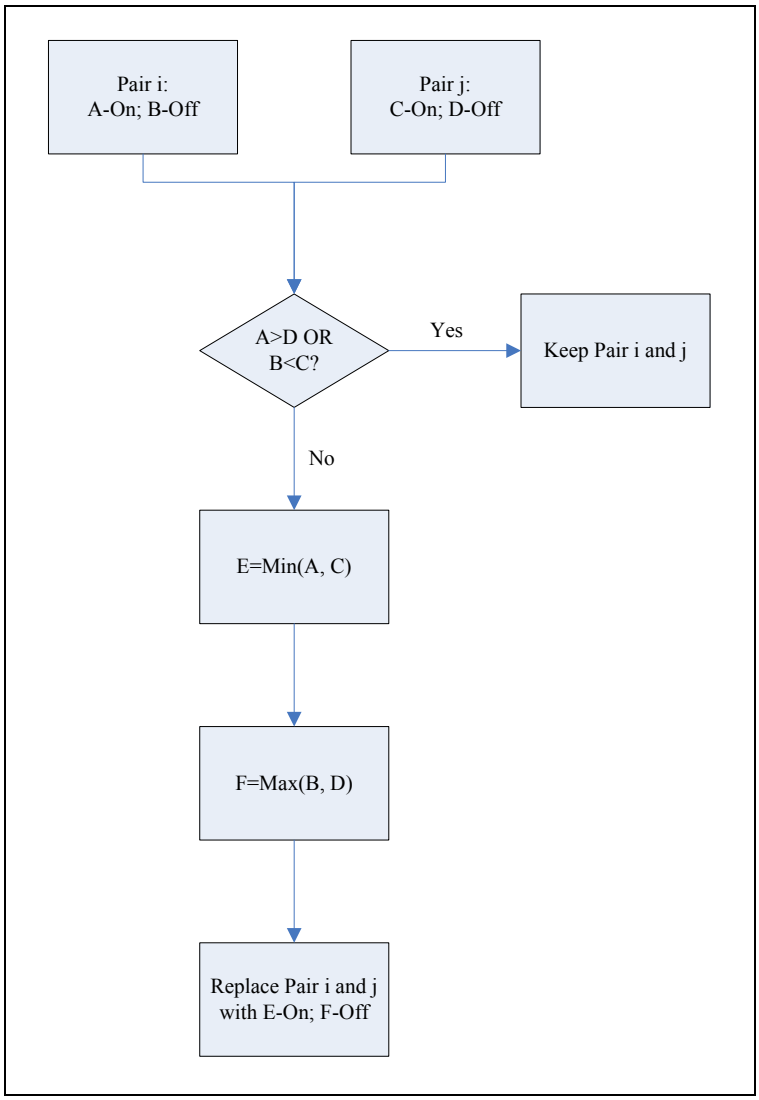

Figure 3 - 5 Flowchart of Union Operation between Control Point Pairs

For example, as seen in Figure 3-6, within a single stoke, there are three search lines: each bold section represents an ON-OFF control pair of spray.

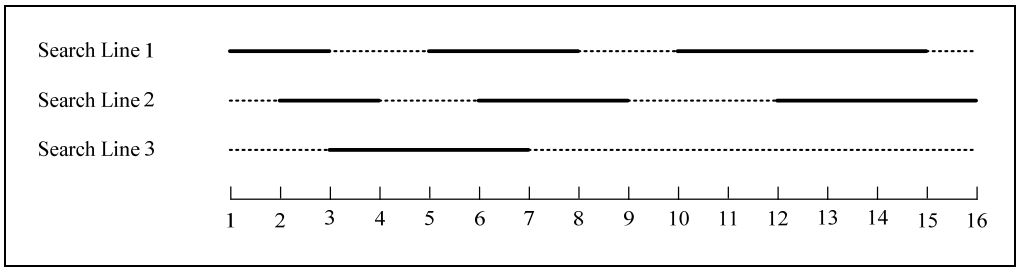

Figure 3 - 6 Uncombined Search Lines and Control Pairs (Bold Sections)

The control points' coordinates and status are given in Table 3-4.

Table 3 - 4 Uncombined Control Pairs

Search Line 1	1	3	5	8	10	15
	ON	OFF	ON	OFF	ON	OFF
Search Line 2	2	4	6	9	12	16
	ON	OFF	ON	OFF	ON	OFF
Search Line 3	3	7				
	ON	OFF				

Combining the control coordinates and the status of Search Line 1 with Search Line 2 generates the intermediate results as shown in Figure 3-7 and Table 3-5. Further combining Search Line 1&2 with Search Line 3 generates the final results as shown in Figure 3-8 and Table 3-6.

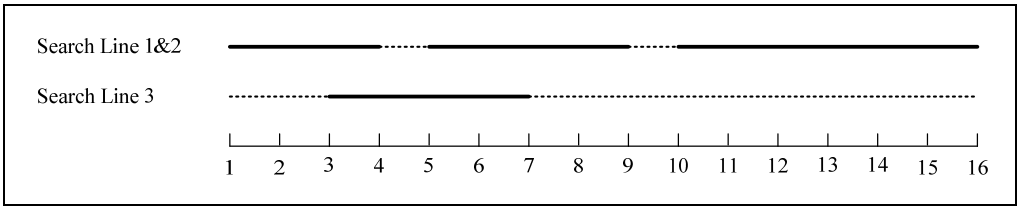

Figure 3 - 7 Combining Search Line 1 and 2

Table 3 - 5 Remaining Control Pairs after Combining the First Two Search Lines

Line 1&2	1	4	5	9	10	16
	ON	OFF	ON	OFF	ON	OFF
Line 3	3	7				
	ON	OFF				

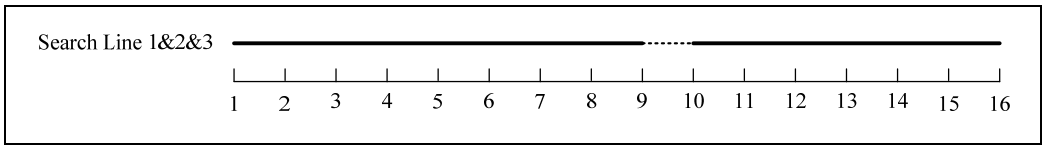

Figure 3 - 8 Combining Search Line 1, 2 and 3

Table 3 - 6 Final Result of Spray Control within a Single Gun Stroke

Line 1&2&3	1	9	10	16
	ON	OFF	ON	OFF

3.2.6 Determining the number of the paint gun strokes

As suggested by Talbert [16] the overlapping distance between neighboring strokes should be kept at the radius of a spray spot. Let Δy be the span of the target surface in Y direction and r be the radius of the spray spot. The number of strips or gun

strokes N should be:

$$\frac{\Delta y}{r}+1 \le N < \frac{\Delta y}{r}+2,$$

where N is an integer, and

$$\Delta y = y_{\max} - y_{\min}$$

By setting the center line of a strip to $y_{\min}$, and performing N strokes in stepped form, the surface will be covered.

3.2.7 Control points adjustments and gap analysis

As the X-Y path planning is to be planned as a stepped form, among the N strokes, for odd-indexed ones the direction of the motion the paint gun is forward, and for the even-indexed strokes, the direction is backward, which is different from the generation of control points' status, which are solely planned in ascending order of X coordinates. Thus the control points' sequence and status should be adjusted accordingly.

1) During the forward movement, the sequence and status of control points should be kept as generated in Section 3.2.5.
2) During the backward movement, the sequence of control points should be in descending order, and the corresponding status generated should be inversed.

To ensure a uniform thickness of paint at the boundaries, spray should be turned on before entering a target region and turned off after leaving it by a distance of r, which is the radius of a spray spot. Thus the following adjustments should be applied:

1) During the forward movement, the ON control points' X coordinates should be decreased by r and OFF control points' X coordinates should be increased by r.

2) During the backward movement, the ON control points' X coordinates should be increased by r and OFF control points' X coordinates should be decreased by r.

A special case of "bridging" may happen during the coordinate adjustment. Suppose the neighboring OFF-ON points' coordinate are X_i and X_{i+1} respectively, if $X_{i+1} - r \le X_i + r$, i.e. $X_{i+1} - X_i \le 2r$, these OFF, ON control points should be deleted, because the gap between them is too small to perform an OFF-ON cycle.

3.3 Three Dimensional Scanning Based Path Planning

3.3.1 General description

Previous sections were aimed at planning spray controlling based on the 3D freeform surface's projection onto the XY plane. In this section, the method is further developed to be capable to perform a spray painting path planning on the actual 3D surface, and still guarantees a full coverage and keeps the maximum possibility of a uniform thickness.

To perform a comprehensive 3D spray painting path planning, eight factors should be determined, including the coordinates of spray cone center and direction of the paint gun in terms of, α and β. The α and β are the rotation angle in the Y-Z Plane (roll angle) and X-Z Plane (yaw angle), respectively. The rotation angle in X-Y Plane will not be considered, as the spray spot is a circle, and is symmetric about the Z axis. Gun distance is the measurement of length between the center of the spray cone at the surface and the gun tip, which affects the coverage area of the painting finish. Moving speed is the one for the spray spot, relative to the target surface. The final factor is the ON-OFF control, which determines the spray status, and could help minimize the waste of painting material.

Determination of X, Y, ON-OFF Status was done in the 2D planning stage, so this section will consider the remaining five factors.

3.3.2 Scanning process

As seen in Figure 3-9, the laser range scanner is attached to the X-Y mechanical stage to perform a stepped motion.

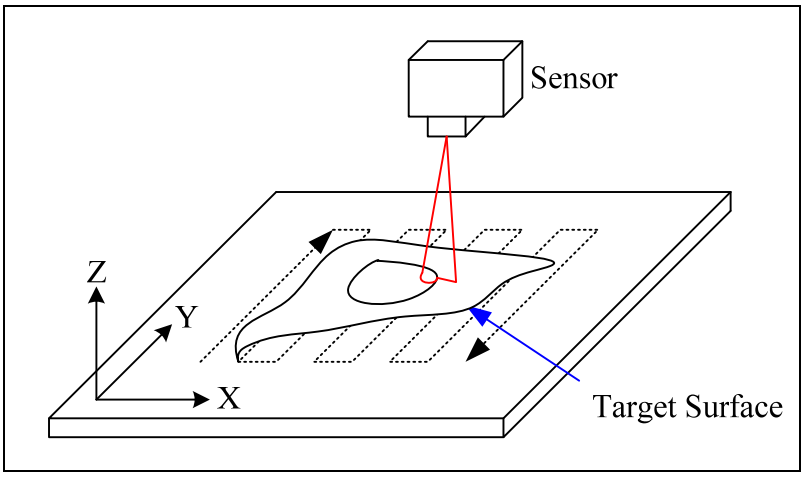

Figure 3 - 9 Laser Range Scanning

The parameters are set as follows:

1) Scanning region – defined by the physical location of the target surface, which is identified during the image acquisition step. It is a rectangular region within four vertices: (x_{min} , y_{min}), (x_{min} , y_{max}), (x_{max} , y_{min}), and (x_{max} , y_{max}).
2) Depth threshold – measurement deeper than this value will be considered as no target surface at current point, and therefore will not be painted.

Scanning results:

By a stepped motion of the laser ranger scanner, the target surface will be described by a cloud of points.

3.3.3 3D surface patching

In order to facilitate the 3D planning procedure, the point cloud will be preliminarily processed by the system. Since it is quite possible that the target surface has holes, and its boundary is irregular, the input point cloud would be viewed as unevenly sampled (spacing between neighboring points' X or Y coordinates are not equal). A new 3D surface, which goes through all the points in the cloud, could be mathematically constructed within the rectangular region of A, which is defined as:

$$A = \{(x_i, y_i) : x_{min} \le x_i \le x_{max}; y_{min} \le y_i \le y_{max}\},$$

where x_{min} , x_{max} , y_{min} and y_{max} are the extreme X, Y coordinates in the point cloud, and

x_i's and y_j's are evenly spaced. For the locations where original target surface has holes or irregular boundaries, corresponding locations, z_i's value will be interpolated by cubic B-spline method. In this way, any target surface will be patched to have a rectangular XY projection without holes. As illustrated in Figure 3-10, each point (x_i, y_i, z_i) at the intersection is defined as a sampling point, and a sampling line is formed by connecting the sampling points with the same Y coordinates horizontally.

The paint gun path will be planned in discrete form, stroke by stroke, and within each stroke, steps are generated according to infinitesimal sections of the target surface. An infinitesimal section is defined as the portion of the target surface, whose XY projection is within a given stroke and located at the small neighborhood around the line that is connected by sampling points with the same X coordinates. (See Figure 3-10.)

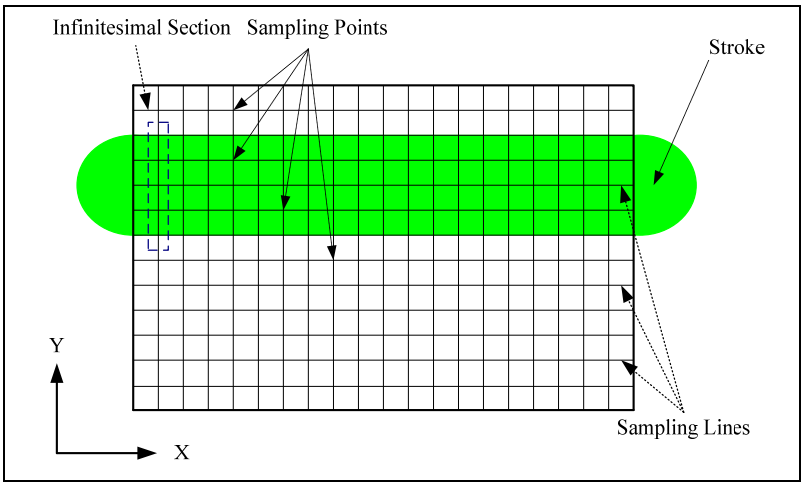

Figure 3 - 10 XY View of the Patched Surface

3.3.4 Spray center's Z coordinate, gun's roll angle, distance and speed

Figure 3-11 is the side view of an infinitesimal section of the target surface from the Y-Z plane. For an infinitesimal section of a strip along the X direction, it could be approximated as a straight line that is connected by the two end points (x_1, y_1, z_1) and (x_3, y_3, z_3) in the 3D space. The spray center's Z coordinate z_2 is calculated as:

$$z_2 = (z_1 + z_3)/2 \quad \text{.....1}$$

When $z_1 \neq z_3$, as seen in Figure 3-11, in order to cover the inclined surface, the required diameter of the new spray cone should be

$$D' = D / \cos\alpha \quad \text{.....2}$$

where D is the original spray cone diameter for the planning on X-Y Plane, and α is given by:

$$\alpha = \arctan[(z_3 - z_1)/(y_3 - y_1)] \quad \text{.....3}$$

The gun distance should be changed to L' to adapt to this new diameter. As

$$D = 2L \times \tan\theta \quad \text{.....4}$$

where θ is the spray angle, and is an inherent gun parameter. By equation 1 and 2, the relationship between the new and original gun distance is:

$$L' = L / \cos\alpha \quad \text{.....5}$$

By changing the gun distance, the full coverage could be ensured, since the uniformity of thickness ultimately relies on the painting velocity. As suggested by Chen [5], the painting thickness is inversely proportional to the painting velocity:

$$V_1 \times T_1 = V_2 \times T_2 \quad \text{.....6}$$

where V_1, T_1, V_2, T_2 are two motion speed and thickness sets, respectively. Because

$$A = \pi \times D^2 / 4 \quad \text{.....7}$$

where A is the spray cone area. Also, according to Suh [1], the spray area is inversely proportionally to the painting thickness, thus:

$$A \times T = A' \times T' \quad \text{.....8}$$

From Equations 1, 2, 5, and 6, at the new gun distance L', and original motion speed, the painting thickness is found as follows:

$$T' = T \times \cos^2\alpha \quad \text{.....9}$$

From equation 4, allowing $V_2 = V, T_2 = T', T_1 = T$, and then the new motion speed to achieve the original thickness should be:

$$V' = V \times \cos^2\alpha \quad \text{.....10}$$

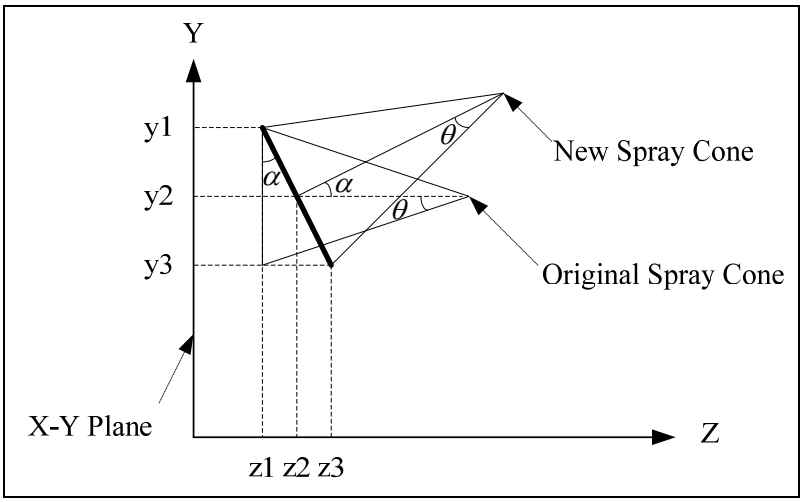

Figure 3 - 11 YZ View of an Infinitesimal Section

3.3.5 Spray gun's yaw angle

For each infinitesimal section of the target, a paint gun's yaw angle (β) could be determined by:

$$\beta = \sum_{i=1}^{N} \beta_i / N$$

$$\beta_i = \arctan(u_i / w_i)$$

where u_i is the target surface's normal vector's projection on the X direction at the sampling point (x_i, y_i, z_i), and w_i is the one on the Z direction (See Figure 3-12.); N is the total number of sampling points within the infinitesimal section. For example, in Figure 3-10, at the circled infinitesimal section, N=5.

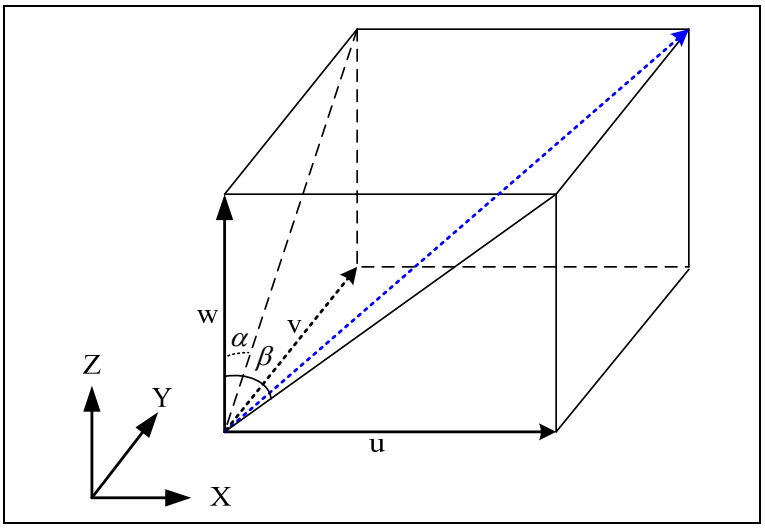

Figure 3 - 12 Decomposition of a Normal Vector

Thus far, the generation of all the factors of comprehensive path planning for 3D

spray painting have been determined. However, in order to make the whole algorithm more robust and practical, more special conditions should be considered and are introduced in the following sections.

3.3.6 Planning on the boundary and lead-lag zones

1) Boundary zone planning

In order to have a full coverage, the final gun stroke will almost always go out of the target surface, and the region outside the XY projection of the target surface is defined as the boundary zone, as shown in Figure 3-13.

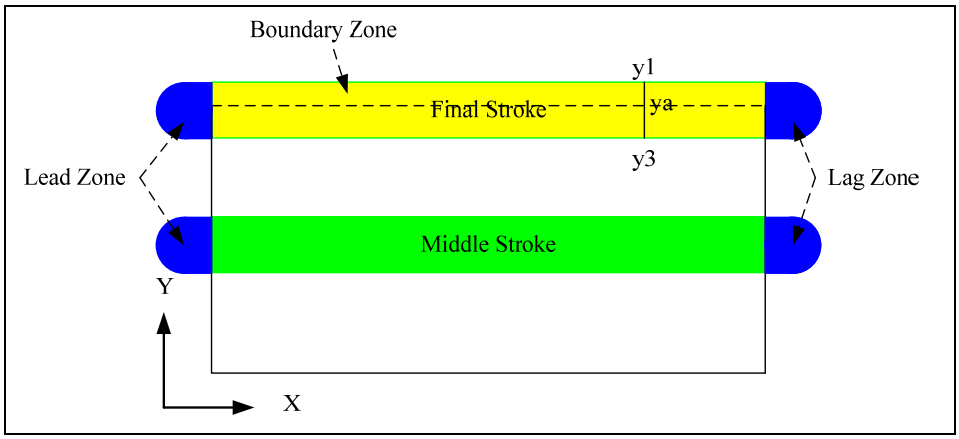

Figure 3 - 13 Boundary, Lead and Lag Zones

A feature and also a disadvantage of the boundary zone is that part of the z coordinates could not be measured by the laser range scanner at the location where there is no material for the surface, which will bring difficulty in doing the computations for the spray cone center's z coordinate, the roll angle, and all the other quantities described in Section 3.3.4, since z_1 does not exist. The following method should be applied in such a situation.

In Figure 3-14, the inclined bold line represents an infinitesimal section of a stripe, similar to Figure 3-11. The difference is that the end points' Z coordinate could not be measured by the laser scanner; since there is no material for that part of the surface (dotted sections are no-material regions). With the knowledge of the extreme measurable points (y_a, z_a), the coordinate of z_1, spray cone center z_2 and the roll angle α could be calculated.

$$\alpha = \arctan(\frac{z_a - z_3}{y_a - y_3})$$

From the geometry relationship, we have:

$$\tan\alpha = (z_a - z_1)/(y_a - y_1)$$

Rearrangement of the equation generates:

$$z_1 = z_a - \tan\alpha \times (y_a - y_1)$$

Then, by adapting equations in Section 3.3.3, the factors for 3D spray painting planning could all be determined.

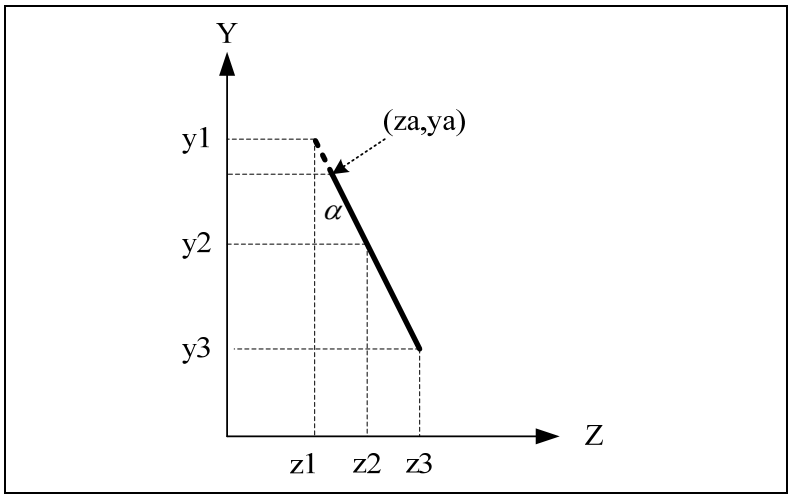

Figure 3 - 14 Planning for Boundary Zone

2) Lead and lag zone planning

As seen in Figure 3-13, the feature of the lead and lag zones is that the target surfaces within do not contain any material at all, whose purpose is to guarantee a uniform thickness at the left and right boundaries. Planning of the start point of a stroke is calculated by linear extrapolation of the first and second sampling points toward the outside by a distance with X component equal to the spray radius. As illustrated in Figure 3-15, the coordinate of the start point is given by:

$$x_0 = x_1 - r$$

$$z_0 = z_1 - r \times \tan\delta$$

$$\delta = \arctan[(z_2 - z_1)/(x_2 - x_1)]$$

The gun direction at the start point should be the same as the one at the first

sampling point in order to have a smooth entering to the surface.

Planning in the lag zone for the coordinate of the stop point within a gun stroke could be done in the similar way by linear extrapolation of the last and second to the last sampling points toward outside the target surface.

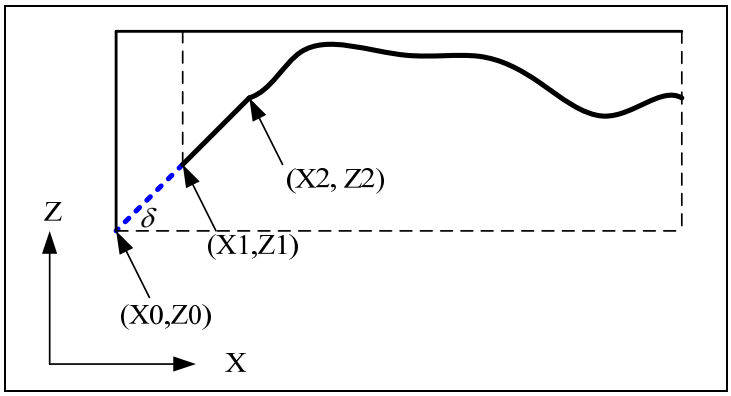

Figure 3 - 15 Planning for Lead Zone

3.3.7 Trimming of the 3D path according to 2D planning result

Since the 3D planning is based on the patched target surface, with the outside boundary of rectangular XY projection. In order to be adaptive to irregular outside boundaries, the 3D path has to be trimmed according to the 2D path, which is planned based on the actual target surface's XY projection. The trimming process is realized by the following steps:

1) For each 2D path, identify the X coordinate of the first ON control point x_a, and the X coordinate of the last OFF control point x_b.

2) On the corresponding 3D path, only the section with X coordinates x_i satisfying $x_a \le x_i \le x_b$ should be kept.

3) Re-connect the remaining sections gives the final 3D path.

CHAPTER 4 RESULTS

The method described in the previous chapter was implemented in LabVIEW. Figure 4-1 is the user interface.

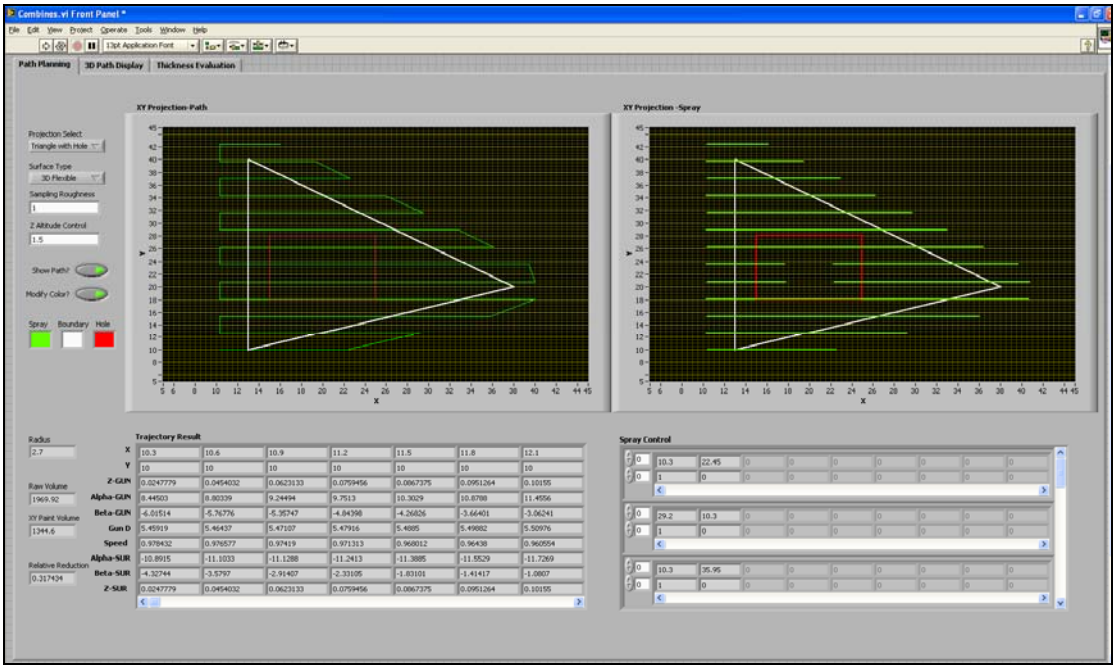

Figure 4 - 1 Software Interface

According to Tank [15], the following parameters were selected for the painting process:

- Spray cone radius: D = 2.7 inches
- Gun distance: L = 5.4 inches

4.1 Path Generation

Four example surfaces were utilized to demonstrate the effectiveness of the automated paint path planning methodologies: plane, partial cylinder, composite surface and 3D arbitrary surface; the generated paths are displayed in Figure 4-2 – Figure 4-5. (Gun directions have also been calculated as part of the trajectory results; however, in order to have a clear display of the gun path, they are not marked on the figures.)

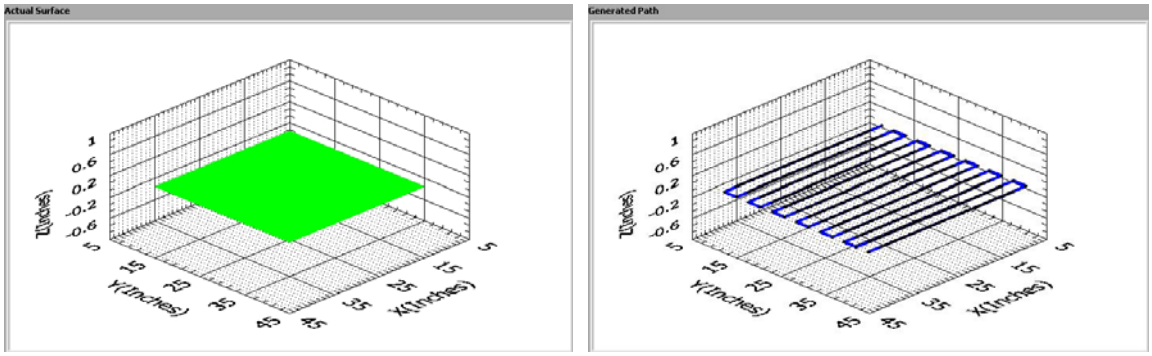

Figure 4 - 2 Target 2D Plane and Path Generated

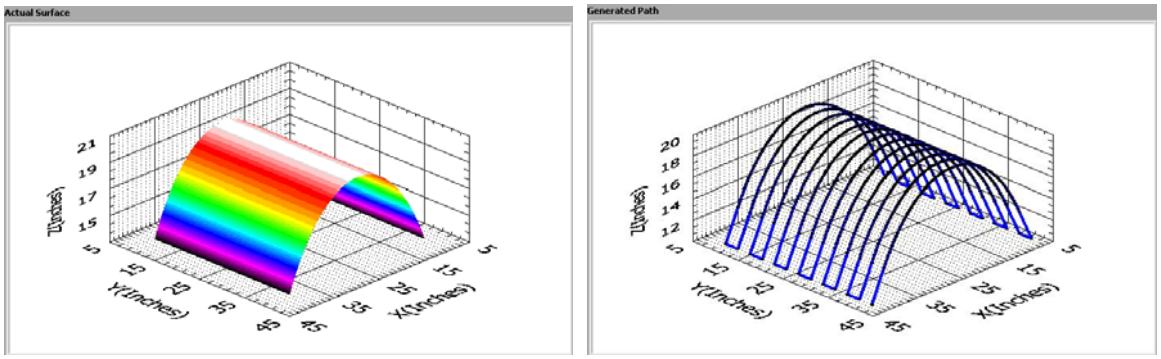

Figure 4 - 3 Target Partial Cylinder and Path Generated

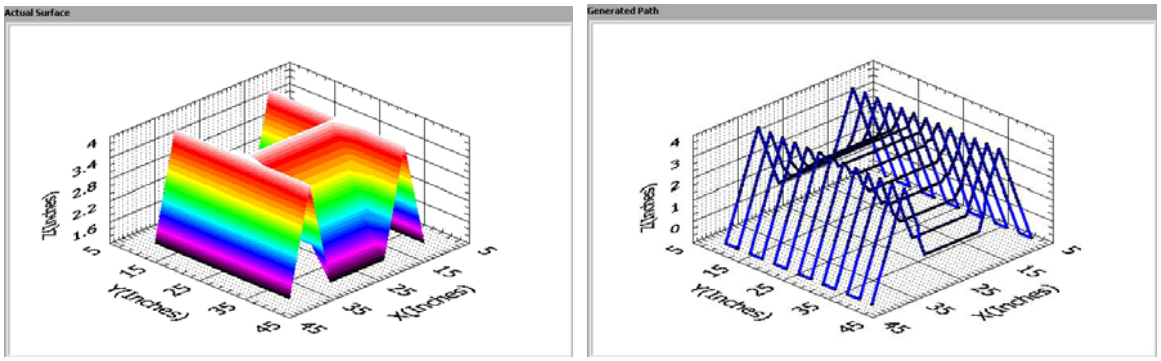

Figure 4 - 4 Target Composite Surface and Path Generated

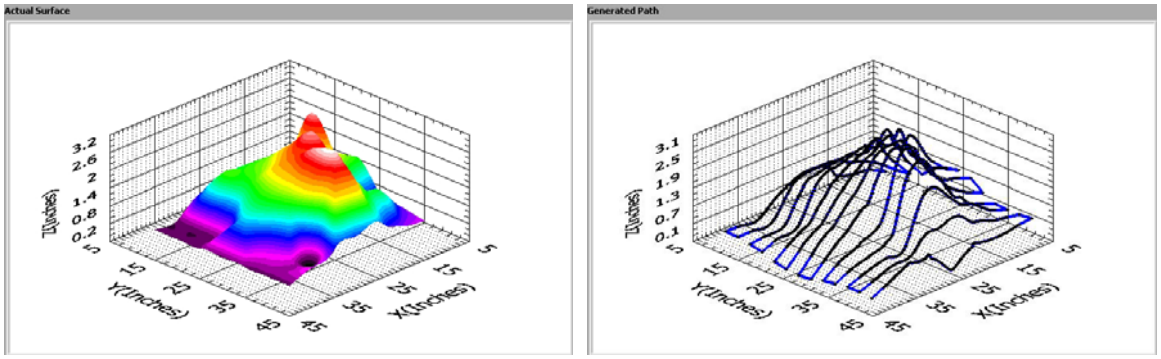

Figure 4 - 5 Target 3D Arbitrary Surface and Path Generated

4.2 Path Planning and Spray Control on Complex Surfaces

In practice, most of the target surfaces will be of irregular shape and possibly contain holes. An XY projection of a surface with triangular shape and a square hole in the middle (See Figure 4-6.) is processed by the software, and the results are shown in Figure 4-7 and Figure 4-8.

Due to the effect of the spray control, paint could be saved by turning off the spray where the path is in a vacant area. Total painting material usage is approximated by multiplying the accumulative length of the ON sections (green sections in Figure 4-8) of the path by the spray cone diameter at the surface. Compared with the traditional methods, which ignores the hole and assumes a rectangular outside boundary, the one proposed in this thesis could save about 32% of paint for this example.

Trimmed 3D paths are shown in Figure 4-10 for the partial cylinder given in Figure 4-9. Figure 4-11 – Figure 4-13 are the trimmed 3D paths for the actual target surfaces, including plane, composite surface and 3D arbitrary surface, respectively, given that the XY projection is of the shape in Figure 4-6.

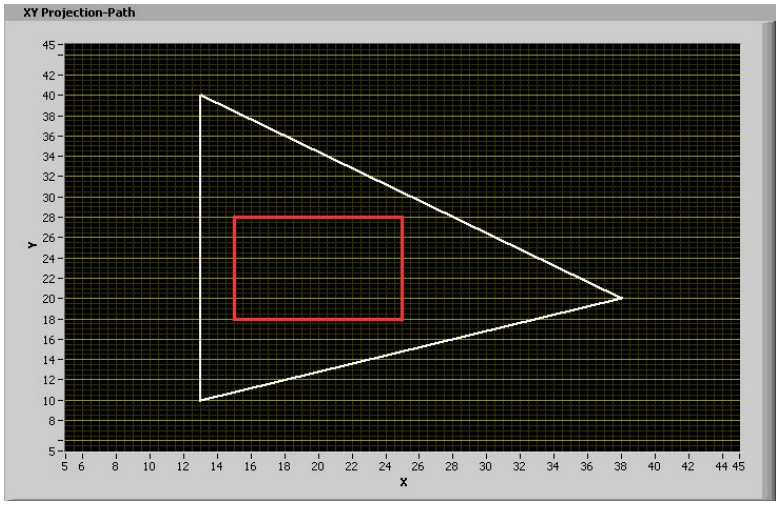

Figure 4 - 6 XY Projection of Target Surface

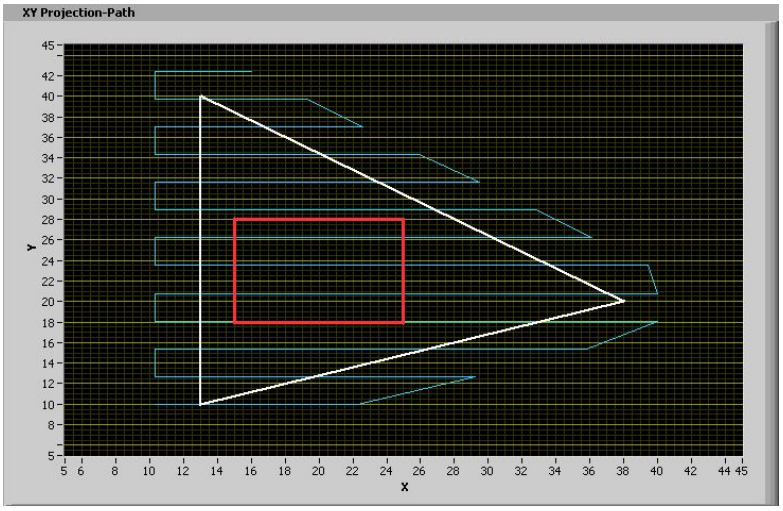

Figure 4 - 7 XY Projection of Planned Path

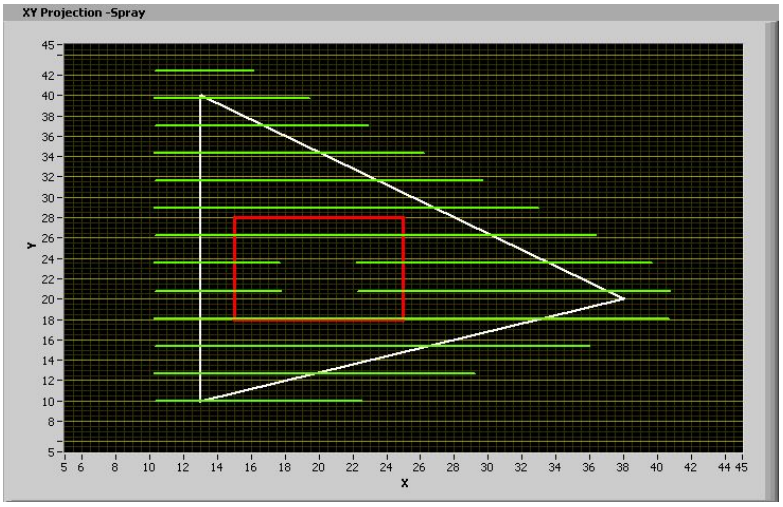

Figure 4 - 8 XY Projection of Spray Control

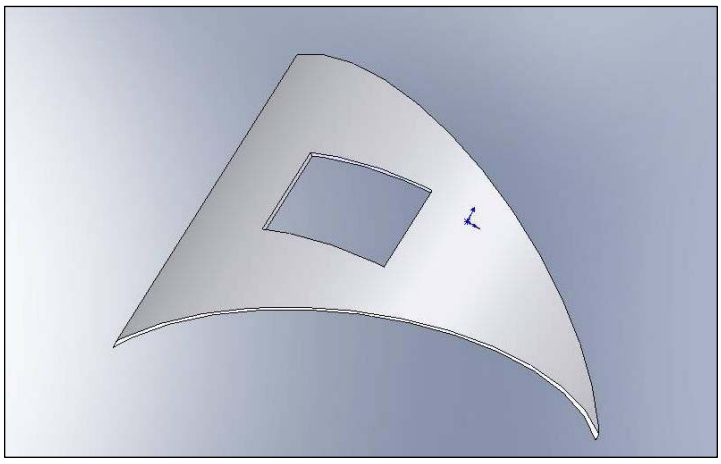

Figure 4 - 9 Partial Cylinder with Triangular XY Projection and a Square Hole

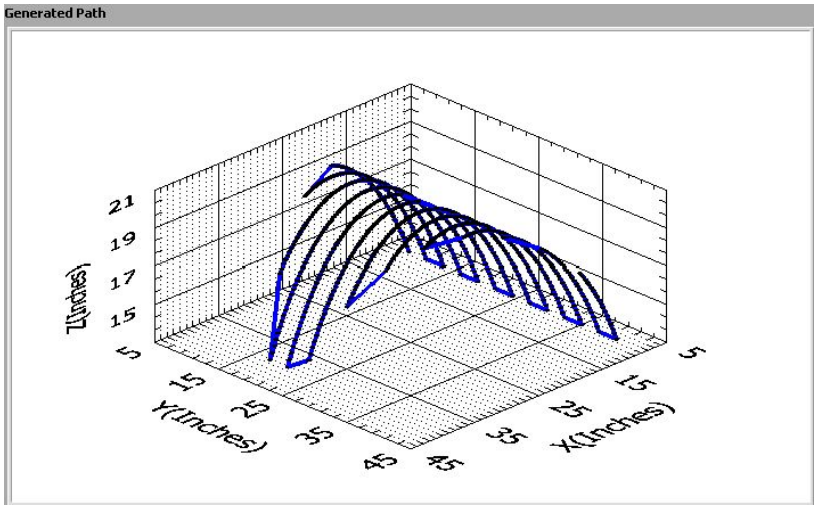

Figure 4 - 10 Trimmed 3D Path of Partial Cylinder

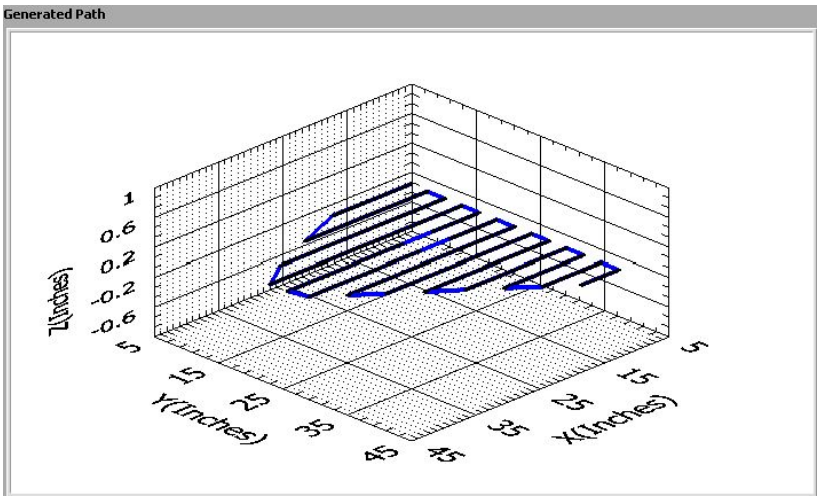

Figure 4 - 11 Trimmed 3D Path of Plane

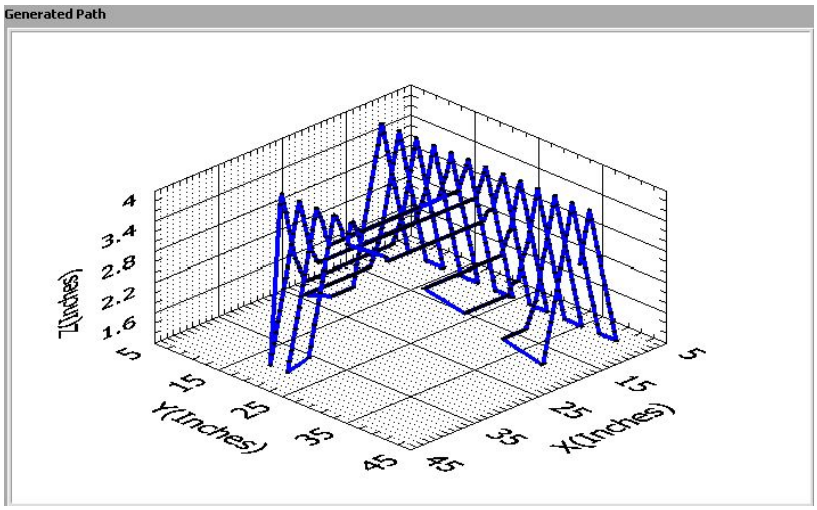

Figure 4 - 12 Trimmed 3D Path of Composite Surface

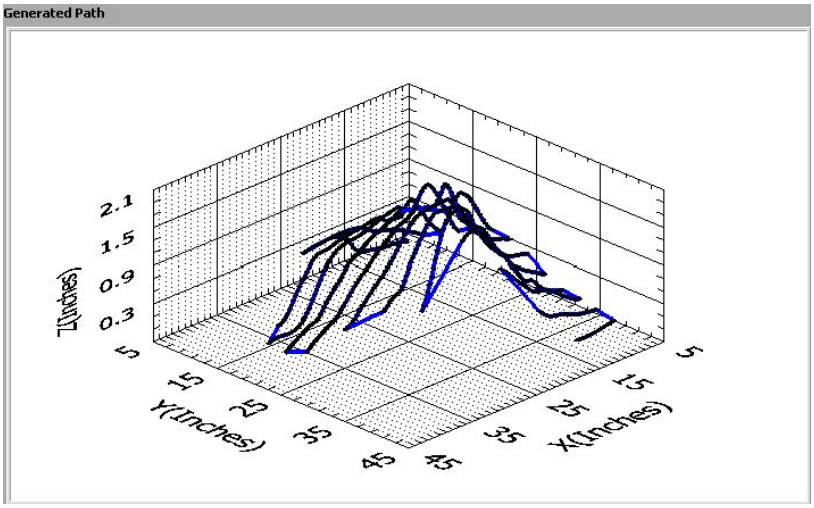

Figure 4 - 13 Trimmed 3D Path of 3D Arbitrary Surface

4.3 Painting Thickness Simulation

To verify the paint thickness across the surface, a simulation method was developed. Meanwhile, paint thickness results are reported numerically and graphically for several examples.

4.3.1 Simulation method

According to the spray painting model established by Suh [1], the spray deposition profile could be described as a semi-ellipse. Since the distance between neighboring paths is equal to the spray radius, the individual deposition profile will be superimposed, as illustrated in Figure 4-14. The numerical relationship among the minimum paint thickness, mean paint thickness and the maximum thickness is given as the ratio: $\delta_{\min} : \delta_{mean} : \delta_{\max} = (2/\pi) : 1 : (2\sqrt{3}/\pi)$.

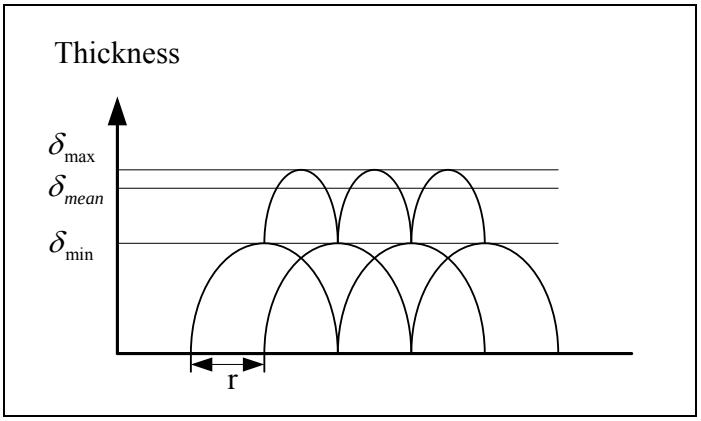

Figure 4 - 14 Superimposed Spray Deposition Profile

Chen [5] provided a simulation method to determine the painting thickness along the gun paths on a freeform surface. The thickness could be determined as:

$$T_s = \overline{T}(L/L_i)^2 \cos\Delta\theta_i$$

Where T_s is the thickness at a sampling point; $\overline{T}$ is the average paint thickness on the virtual plane that is perpendicular to the paint gun's direction at the designed gun distance L; L_i is the projection of actual distance between gun tip and the sampling point onto the gun direction; $\Delta\theta_i$ is the angle between gun direction and the normal direction of the target surface at a given sampling point. Although this is an effective simulation method, it has the limitation of not being able to determine the thickness everywhere on the surface. The sampling points are limited to gun trajectory.

In this work, a new "weighted average thickness simulation method," is developed to make it possible to verify the thickness virtually everywhere across the target surface. For a given point $P(x_0, y_0, z_0)$, with normal direction $[u_0, v_0, w_0]$ on the target surface, it could be located between two neighboring gun paths by satisfying both $y_0 \geq y_i$ and $y_0 < y_{i+1}$, where y_i is the y coordinate for the i^{th} gun path. $P(x_0, y_i, z_i)$ with the gun direction $[a_i, b_i, c_i]$ on the i^{th} gun path has the same X coordinate as the given point $P(x_0, y_0, z_0)$. Likewise, $P(x_0, y_j, z_j)$ is the point on the $(i+1)^{th}$ gun path with the gun direction $[a_j, b_j, c_j]$ on the j^{th} gun path. Here we define $j \equiv i+1$. (See Figure 4-15)

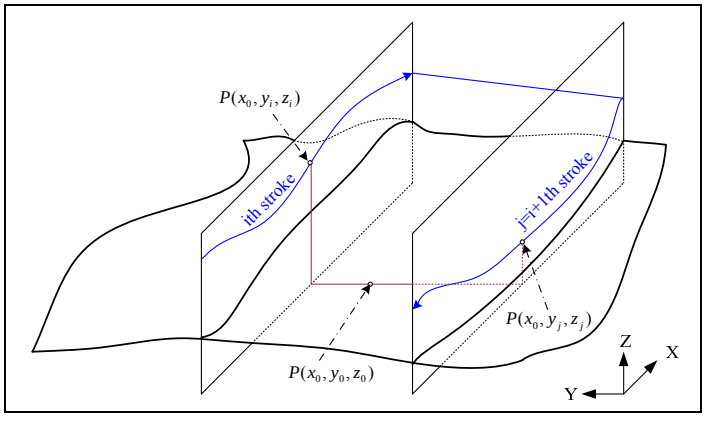

Figure 4 - 15 Locating a Point between Two Gun Strokes

The thickness determined by the i^{th} gun path is $T_i = \overline{T}(L/L_i)^2 \cos\Delta\theta_i$, where

$$L_i = L + \frac{(y_i - y_0)\times b_i + (z_i - z_0)\times c_i}{\sqrt{a_i^{\,2} + b_i^{\,2} + c_i^{\,2}}}$$

$$\cos\Delta\theta_i = \frac{a_i \times u_0 + b_i \times v_0 + c_i \times w_0}{\sqrt{a_i^{\,2} + b_i^{\,2} + c_i^{\,2}} \times \sqrt{u_0^{\,2} + v_0^{\,2} + w_0^{\,2}}}$$

Similarly, the thickness determined by the j^{th} gun path could be calculated as T_j. Then the weighted average thickness considering the effects of both gun paths is given by

$$T_w = \frac{y_j - y}{y_j - y_i} \times T_i + \frac{y - y_i}{y_j - y_i} \times T_j$$

The relative thickness at this point is given as

$$R_w = T_w / \overline{T}$$

In order to be practical, resolution of the laser range scanner is considered in the simulation process in terms of Sampling Roughness Level (SRL), where SRL=N means 1/N of the original points on the target surface could be captured. The process is described in Figure 4-16.

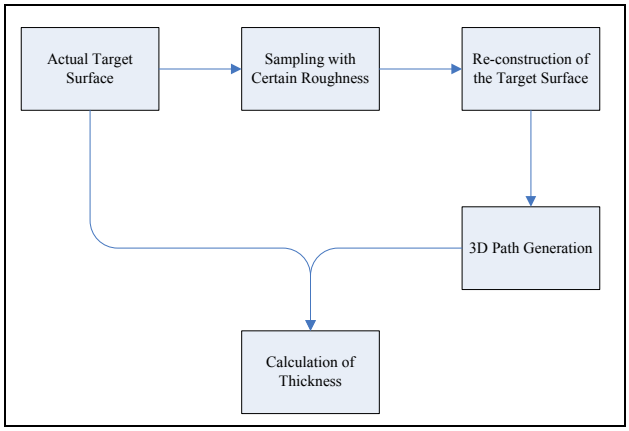

Figure 4 - 16 Flowchart of Simulation Process

4.3.2 Simulation results

Painting thickness for the plane, partial cylinder, composite surface and 3D arbitrary surface were simulated. Three hundred randomly sampled points on the surface were used to communicate the results and are shown for each of the four surface types. Graphical displays of the thickness distributions are also included along with the XY view of the thickness variations. These are shown in Figure 4-17 through 4-37. Also included in this analysis is different SRL's for the partial cylinder, composite surface, and 3D arbitrary surface.

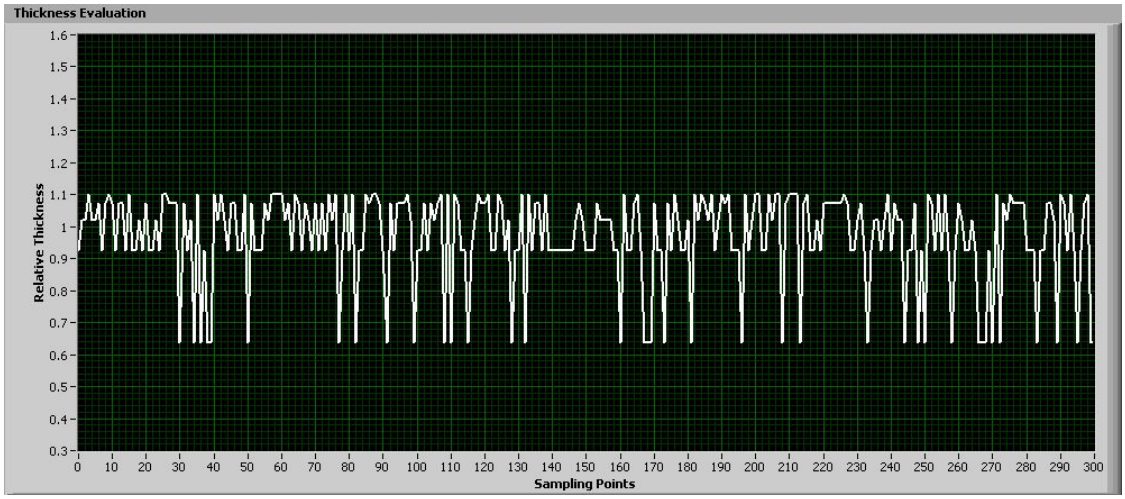

Figure 4 - 17 Paint Thickness on 2D Plane (Numerical, SRL=10)

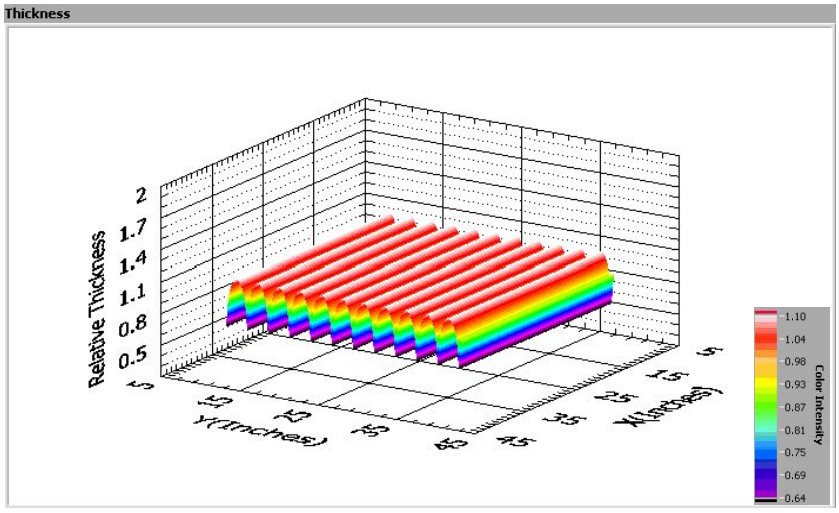

Figure 4 - 18 Paint Thickness on 2D Plane (Graphical, SRL=10)

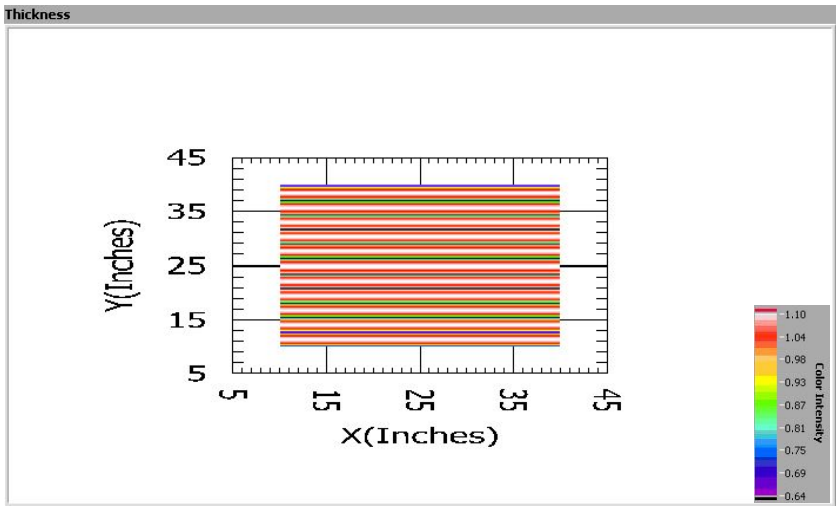

Figure 4 - 19 XY View of Paint Thickness on 2D Plane (Graphical, SRL=10)

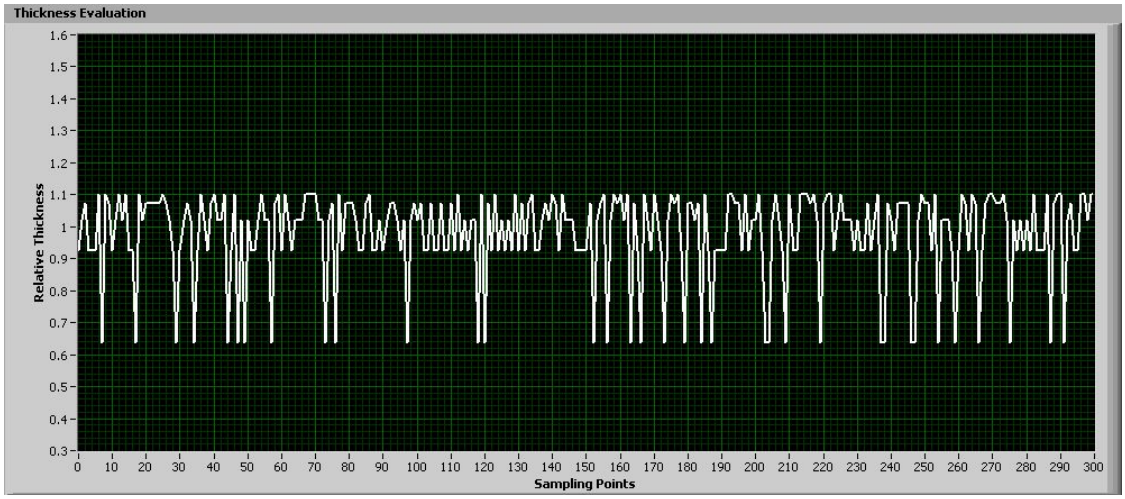

Figure 4 - 20 Paint Thickness on Partial Cylinder (Numerical SRL=1)

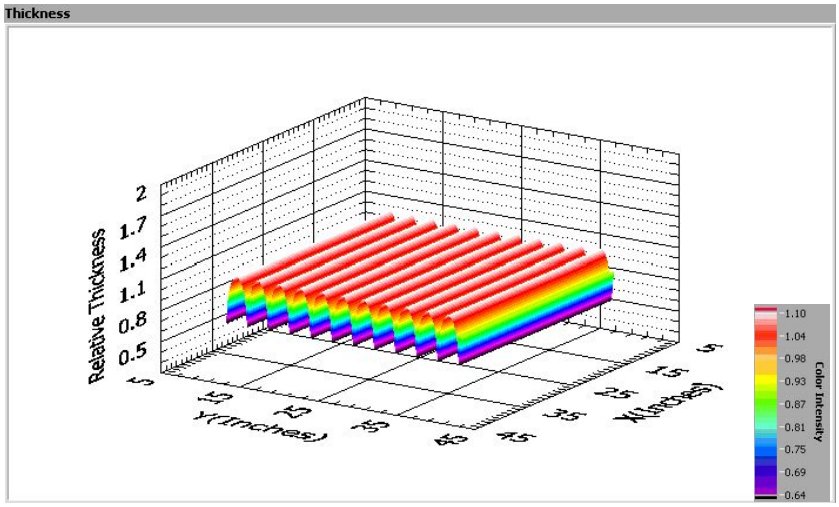

Figure 4 - 21 Paint Thickness on Partial Cylinder (Graphical SRL=1)

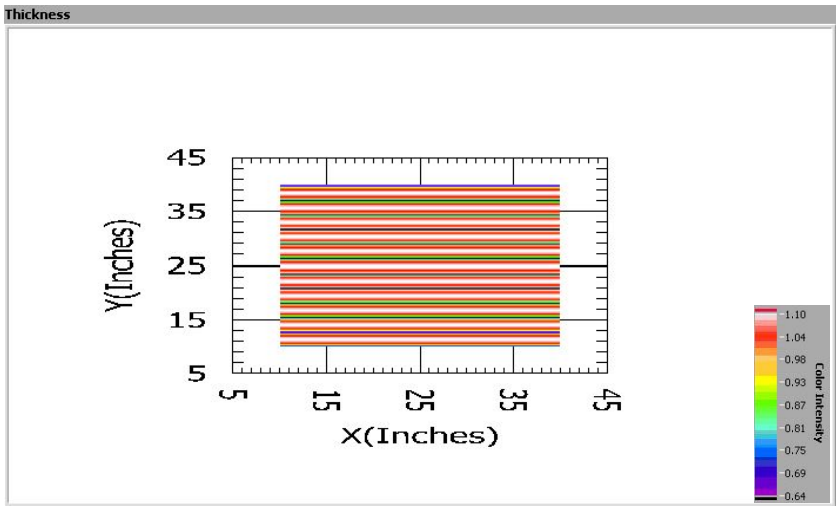

Figure 4 - 22 XY View of Paint Thickness on Partial Cylinder (Graphical SRL=1)

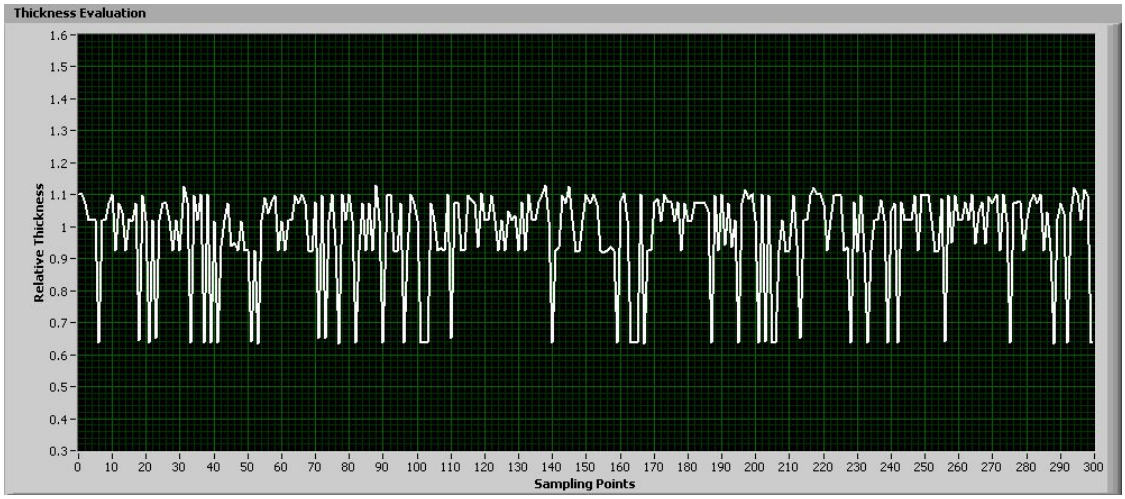

Figure 4 - 23 Paint Thickness on Partial Cylinder (Numerical, SRL=10)

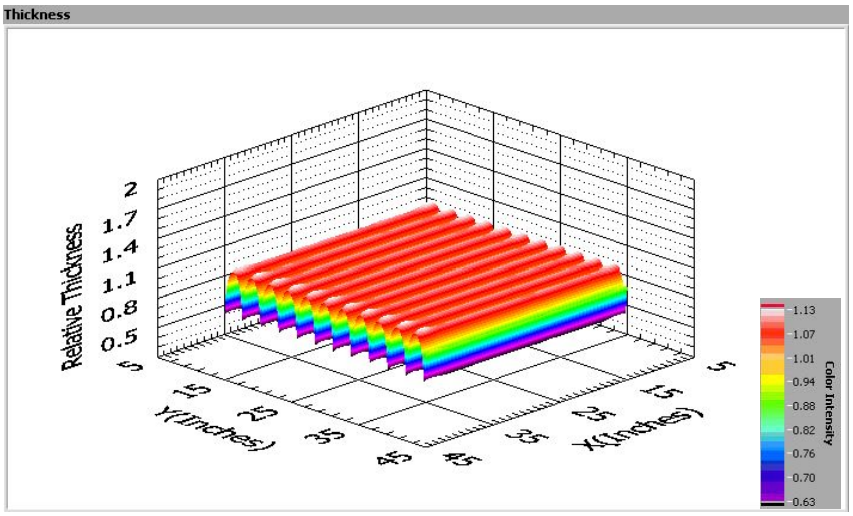

Figure 4 - 24 Paint Thickness on Partial Cylinder (Graphical, SRL=10)

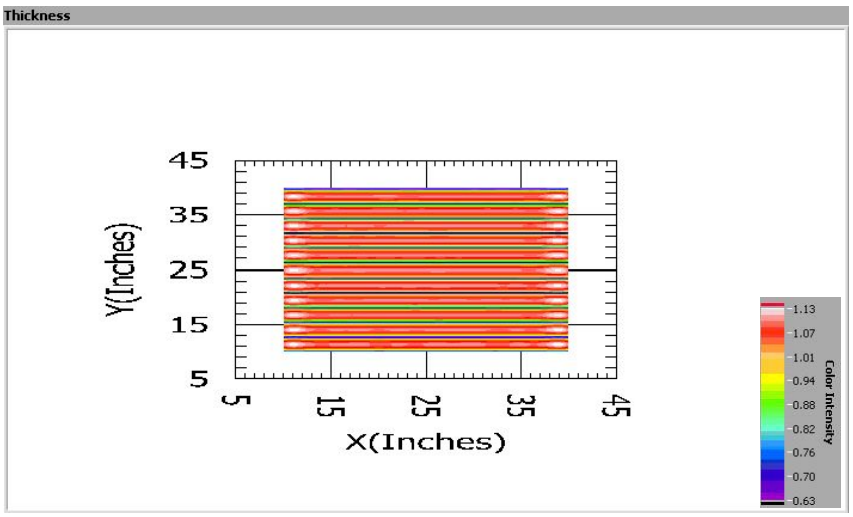

Figure 4 - 25 XY View of Paint Thickness on Partial Cylinder (Graphical, SRL=10)

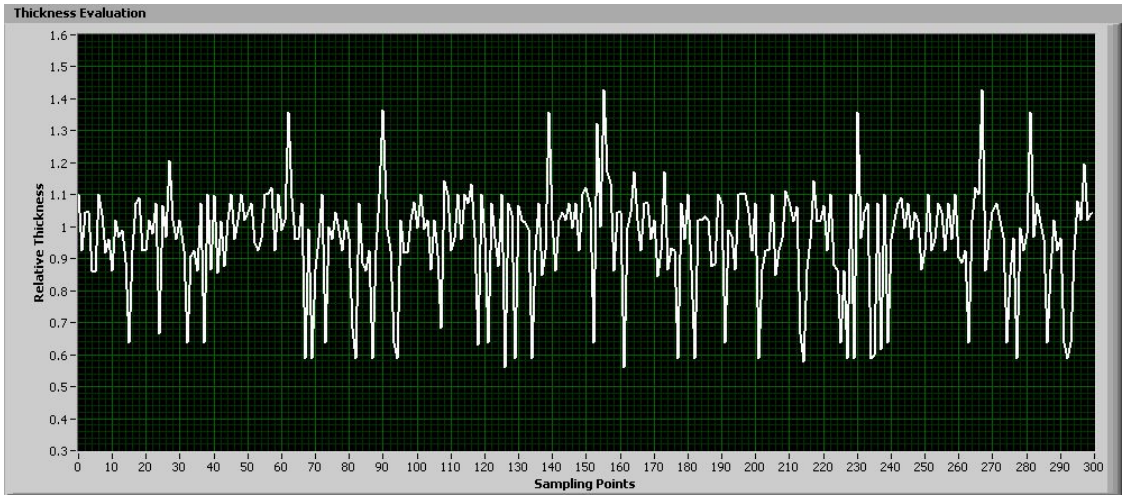

Figure 4 - 26 Paint Thickness on Composite Surface (Numerical, SRL=1)

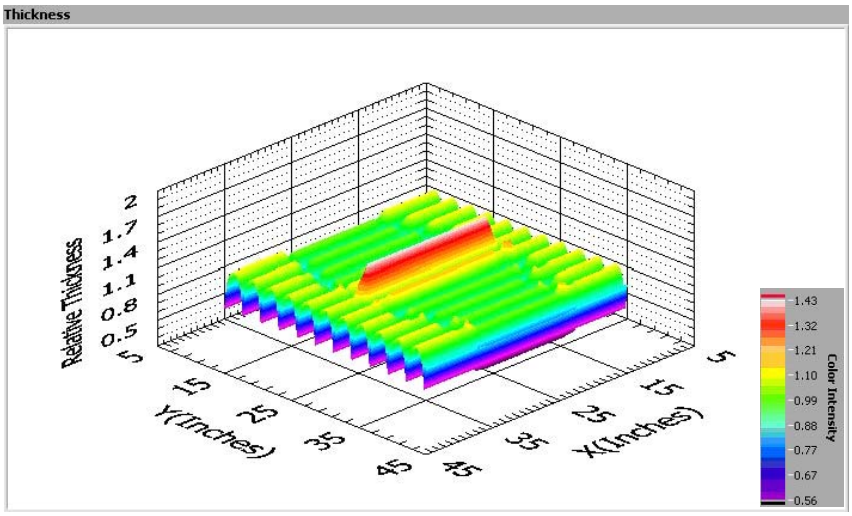

Figure 4 - 27 Paint Thickness on Composite Surface (Graphical, SRL=1)

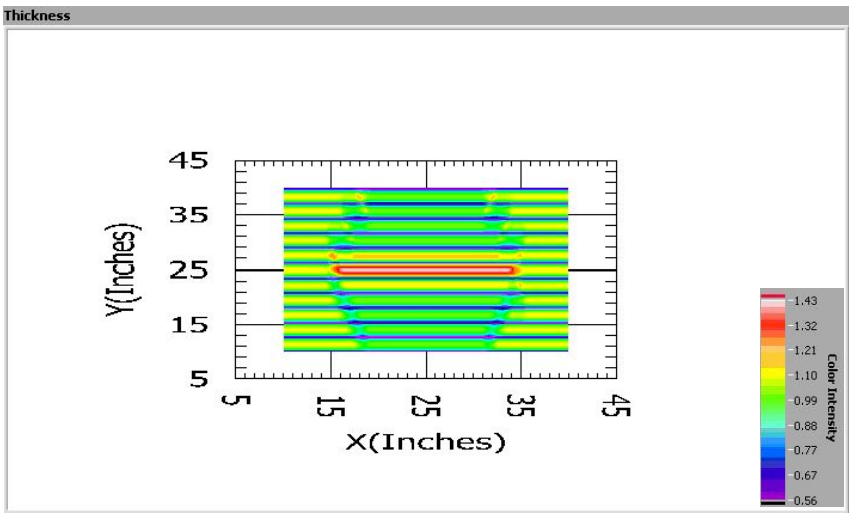

Figure 4 - 28 XY View of Paint Thickness on Composite Surface (Graphical, SRL=1)

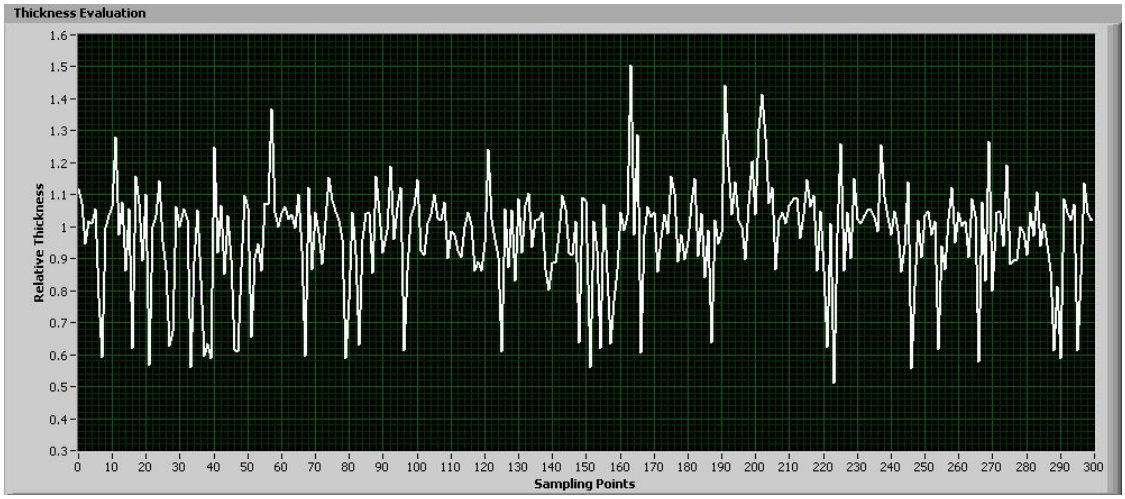

Figure 4 - 29 Paint Thickness on Composite Surface (Numerical, SRL=10)

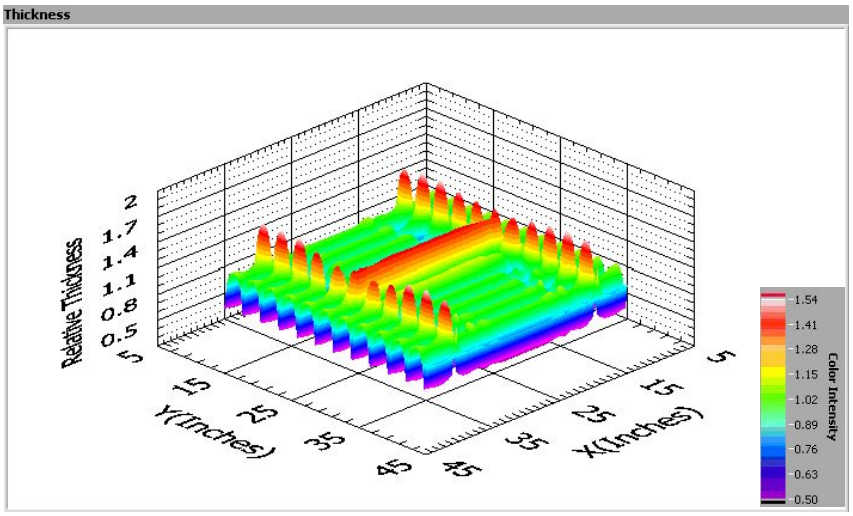

Figure 4 - 30 Paint Thickness on Composite Surface (Graphical, SRL=10)

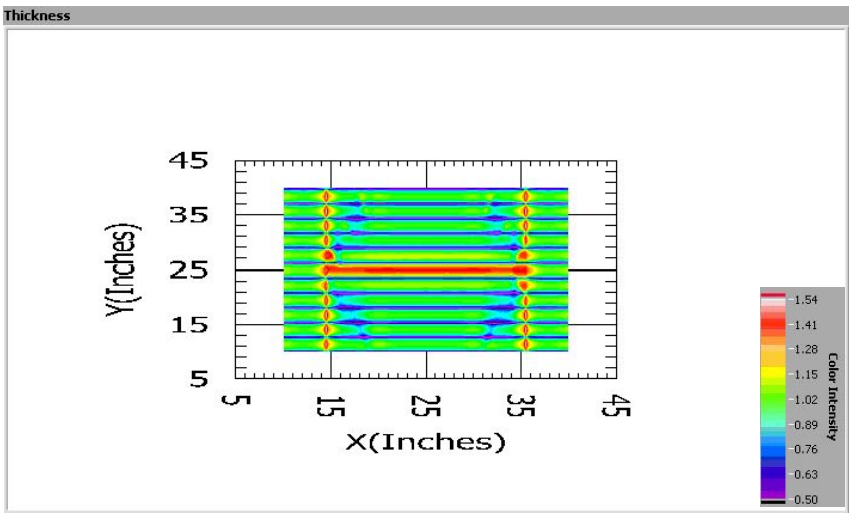

Figure 4 - 31 XY View of Paint Thickness on Composite Surface (Graphical, SRL=10)

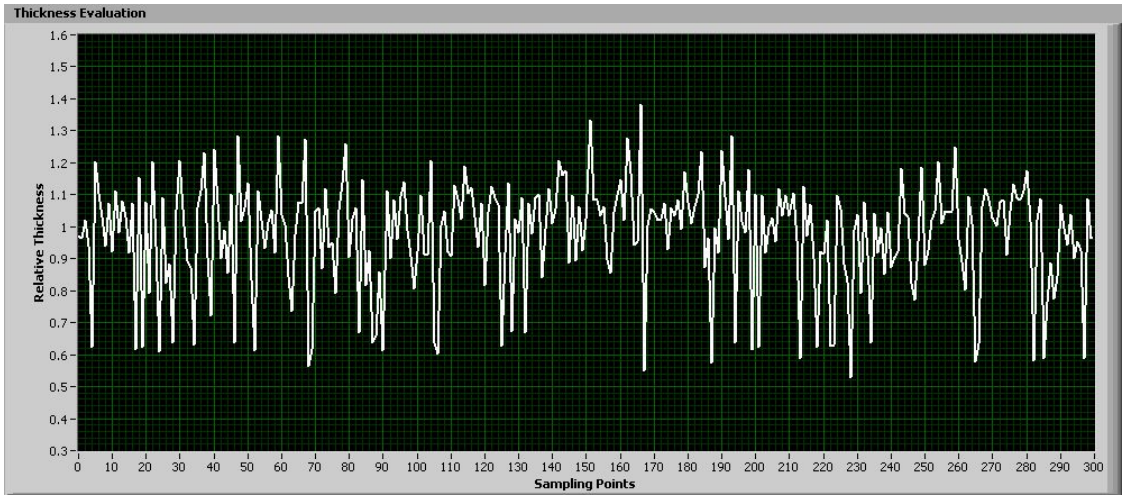

Figure 4 - 32 Paint Thickness on 3D Arbitrary Surface (Numerical, SRL=1)

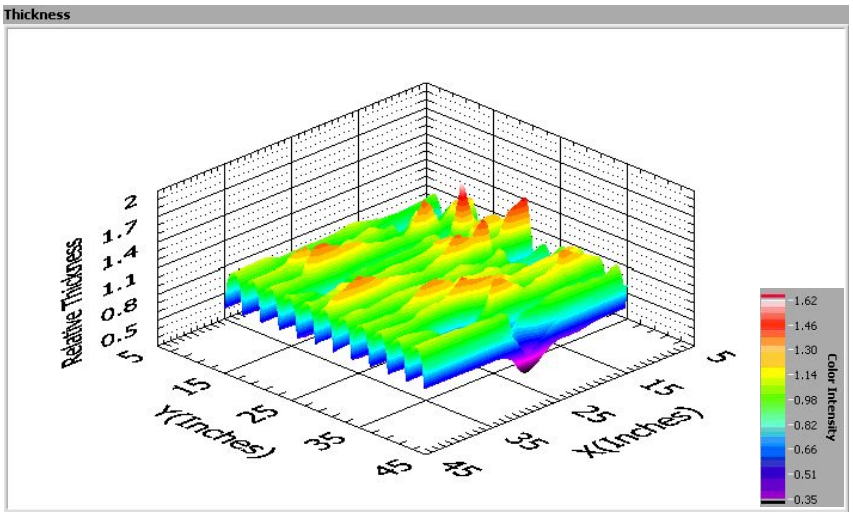

Figure 4 - 33 Paint Thickness on 3D Arbitrary Surface (Graphical, SRL=1)

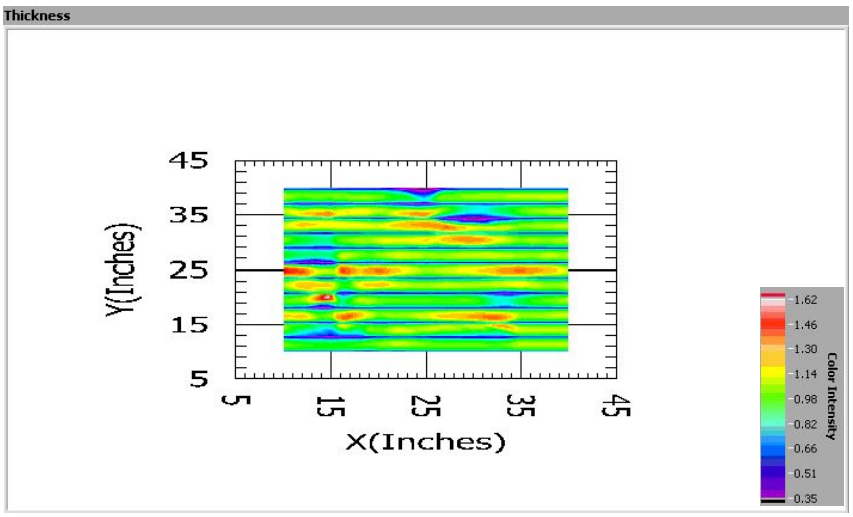

Figure 4 - 34 XY View of Paint Thickness on 3D Arbitrary Surface (Graphical, SRL=1)

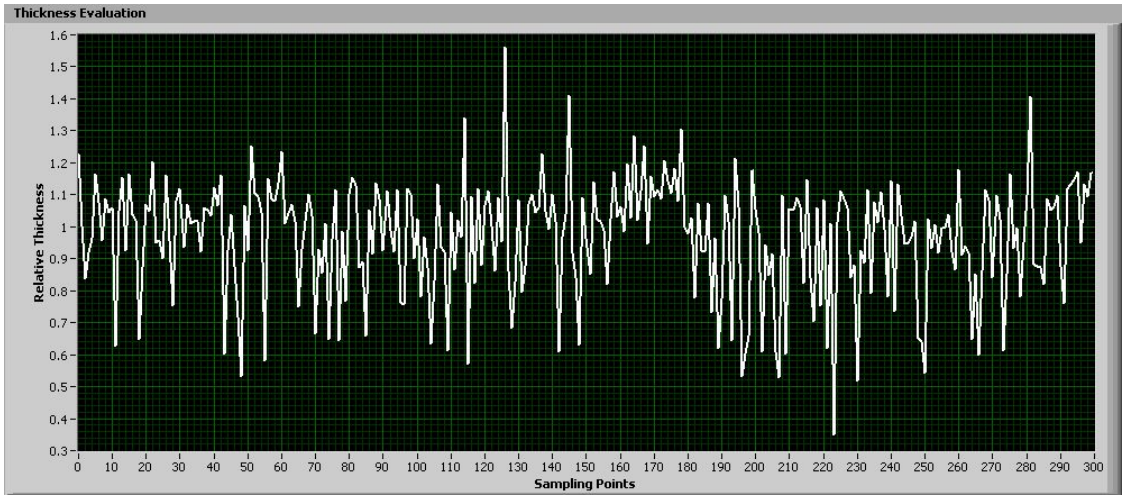

Figure 4 - 35 Paint Thickness on 3D Arbitrary Surface (Numerical, SRL=10)

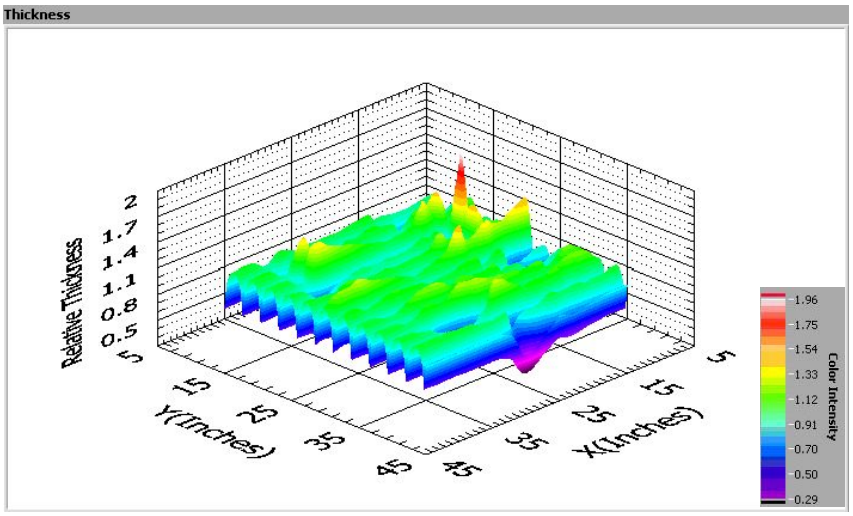

Figure 4 - 36 Paint Thickness on 3D Arbitrary Surface (Graphical, SRL=10)

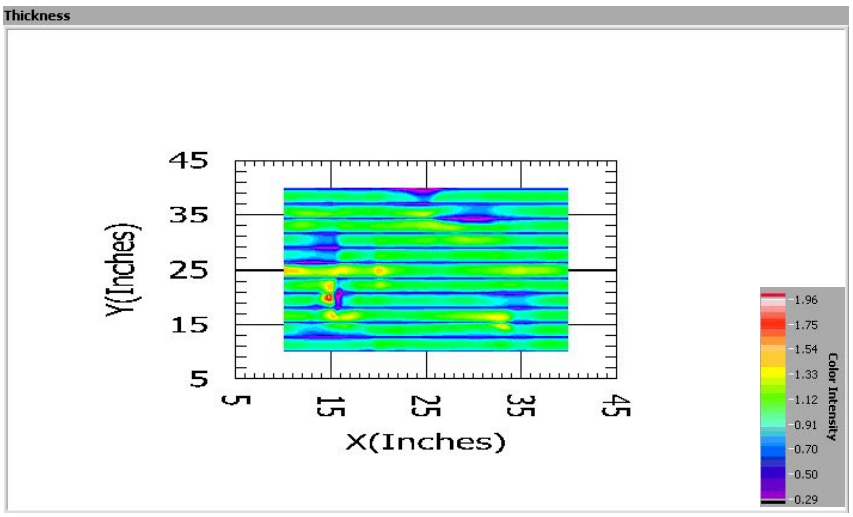

Figure 4 - 37 XY View of Paint Thickness on 3D Arbitrary Surface (Graphical, SRL=10)

The software is also capable of computing the mean and standard deviation of the relative paint thickness for each type of the surfaces in different sampling roughness levels. Summary of the statistics is given in Table 4-1.

Table 4 - 1 Summary of Statistical Results on Relative Thickness

Target Surface	SRL	Mean	Standard Deviation	Range	
2D Plane	10	0.9821	0.1419	0.6366	1.0996
Partial Cylinder	1	0.9821	0.1419	0.6366	1.0996
Partial Cylinder	10	0.9847	0.1425	0.6333	1.1292
Composite	1	0.9674	0.1580	0.5578	1.4263
Composite	10	0.9639	0.1708	0.4979	1.5359
3D Flexible	1	0.9682	0.1735	0.3476	1.6136
3D Flexible	10	0.9686	0.1766	0.2876	1.9563

CHAPTER 5 DISCUSSION

5.1 Coverage and Painting Material Waste Reduction

Since the 3D path generation method is XY projection-based, coverage effectiveness could be checked directly by comparing the XY projection of the target surface and the one for the 3D path. Figure 4-8 shows the target surface with the XY projection of a triangular shape and a square hole. In this example, the green segments representing the center of painting material spray could cover the surface in full. Another feature shown in this figure is that the method could control the spray accurately and adaptively and to the geometry of the XY projection, which minimizes the painting material waste.

5.2 Painting Thickness

For spray painting on the plane, as shown in Figure 4-15, the method could do an acceptable work even at SRL=10. This is because there is no Z coordinate change in either X or Y direction. In this case, the 2D plane could be completely re-constructed during path planning. The only source of thickness variation is from the spray deposit profile (see Figure 4-14), which is of superimposed semi-ellipse shape, rather than a uniform rectangle.

For the straight line based swept surface, as long as the curvature radius is large compared with the spray radius, this method will be acceptable, which is seen in Figure 4-20 – Figure 4-22. In this work, the surface's normal direction is decomposed in to its pitch angle and yaw angle (α and β). Therefore, the paint gun's direction is also planned in a two components manner, where the gun pitch angle planning utilizes the target surface's Z coordinate at the same Y level, and the gun yaw angle is the grand average of infinitesimal surfaces' yaw angles at the same Y level that are covered within the spray cone. In this way, the gun direction could adapt to the curvature change in terms of yaw

angle, and provide an excellent painting finish on the straight line swept surface.

Figure 4-23 shows the paint thickness result for SRL=10. Excess paint around 12.3% is witnessed at a portion of the points. According to Figure 4-25, the location of the excessive painting points are distributed on the left and right edges of the partial cylinder, where the slope changes the most when travelling along the y direction. This error is due to the large sampling roughness: only 10% of the points on the original surface are assumed to be utilized by the planning process.

In cases of path planning on complex 3D surfaces, this method could provide a satisfactory result in terms of painting thickness. For the composite surface, it is seen from Figure 4-26 through 4-28 that for SRL=1, the relative thickness could be controlled within the range of 0.56 to 1.43. From Figure 4-29 – 4-31, it is seen that for SRL=10, the relative thickness range is enlarged, ranging from 0.5 to 1.54.

The reason for poorer performance at the larger SRL value is because that in the rough sampling case, the original target surface could not be adequately re-constructed during the phase of path planning. This is a result of the surface being a combination of several planes intersecting at sharp angles. Since the method uses a Cubic B-spline interpolation method, most of the features will be missed. This can be seen in Figures 5-1 and 5-2; at SRL value of 10, two geometric peaks near X = 15 and X = 35 are missed. Since the path is planned based on this surface, it will have a smaller Z value in these areas, resulting in a closer gun distance to the actual target surface and thus thicker paint. This analysis was verified by the software's numerical result, which indicates that the area of maximum thickness was located at X = 14.5 and Y = 35.5. The model also showed that the minimum thickness happens at X = 32.2 and Y = 15.4, which is in the neighborhood of the intersection line of two planes. The drastic change of the normal directions of local infinitesimal surfaces caused the large difference between the paint gun's direction and the surface's normal direction. According to the simulation model, this was the main reason for the under paint at the measured point.

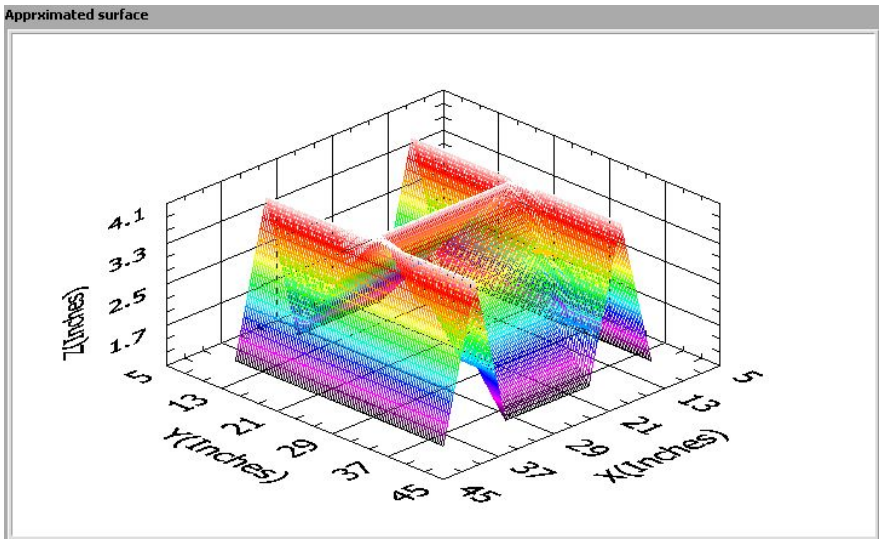

Figure 5 - 1 Re-constructed Composite Surface (SRL=1)

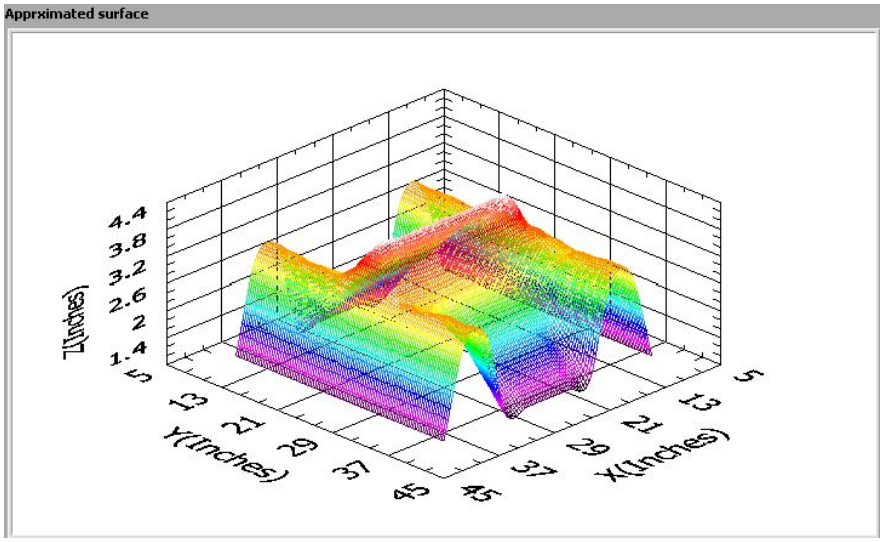

Figure 5 - 2 Re-constructed Composite Surface (SRL=10)

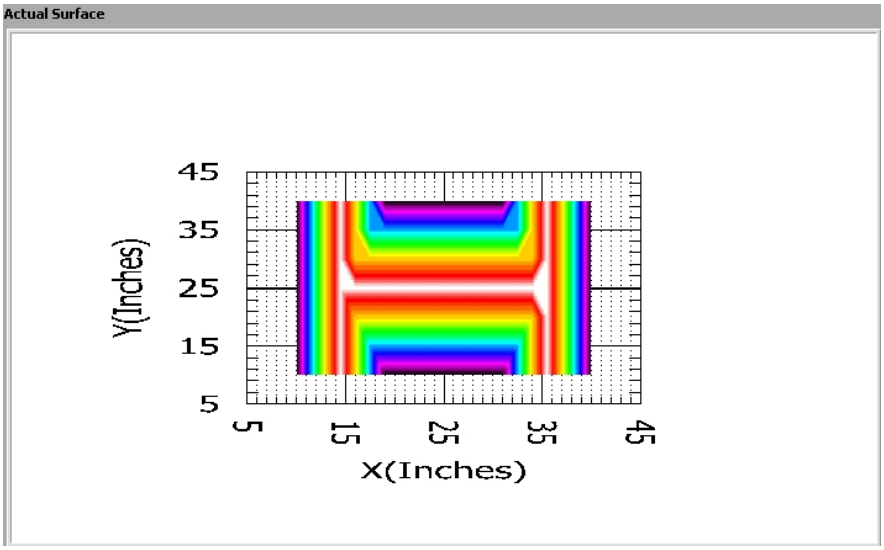

Figure 5 - 3 XY Projection of Original Composite Surface

For the 3D arbitrary surface, at SRL=10, the simulation results showed relative paint thickness between 0.29 and 1.96. This range is wider than the one obtained at SRL=1, which is 0.35 to 1.61. A comparison among Figure 4-34, 4-37 and 5-4 reveals that over painting tends to happen at the geometric peaks, while under painting occurs at the geometric valleys. This is particularly true when the sampling is rough. At a smaller SRL, a large change of slope on the target surface becomes another dominating factor that influences the paint thickness. From the simulation, the extreme under painting point is located at (X=15.7, Y=20.8), and the extreme over paint point is located at (X=14.8, Y=19.9), which is coincide with a huge geometric gradient change from valley to peak. (See Figure 5-4)

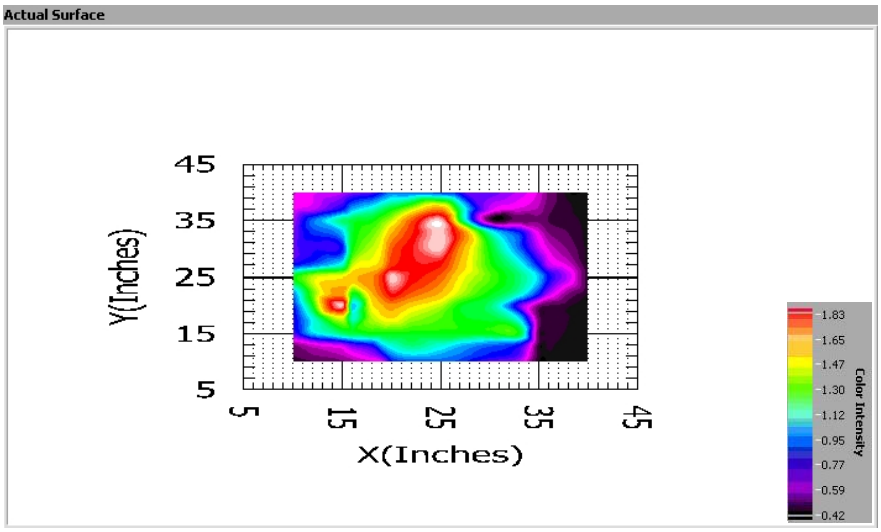

Figure 5 - 4 XY View of the Original 3D Arbitrary Surface

Comparing the painting thickness results on the plane, straight line sweep surface, the composite surface and the 3D arbitrary surface, it is seen that when the target surface is geometrically simple, the dominating factor of thickness variation is the spray deposition profile, which is non-uniform. When the target surface gets complex, the geometric features become another strong factor affecting the thickness variation. Sampling roughness is also a source of the thickness variation, which should be kept as small as possible, especially when the target surface is of complex shape.

CHAPTER 6 CONCLUSION

A new real time system for spray painting planning on unknown 3D surfaces is developed. With machine vision providing the XY projection of boundary loops and the laser scanner providing the point cloud, the system generates paint gun trajectories as well as the control command of the paint spray. Simulation results have shown that the system could perform a full coverage on the target surfaces with irregular boundaries and holes, while keeping the paint material waste at a minimum.

"Weighted average thickness simulation method" has been developed to make it possible to check the thickness across the target surface. Simulation results have shown that the planned gun trajectory could provide an excellent painting thickness on 2D planes and straight line sweep surfaces, and keep the range within ± 65% of the desired thickness in painting on 3D surfaces.

The individual and combined effects of spray deposition profile, sampling roughness level, and target surfaces' geometric features on the relative average painting thickness were analyzed.

Future work will include more analysis on the target surface geometry, orientation control during the painting process to accommodate more complex surfaces.

BIBLIOGRAPHY

1. Suh SH, Woo IK, Noh SK (1991) Development of an automatic trajectory planning system for spray painting robots. Proceedings of the 1991 IEEE International Conference on Robotics and Automation, Sacramento, California, April, pp. 1948-1955
2. Arikan M, Balkan T (2007) Process simulation and paint thickness measurement for robotic spray painting. Mechanical Engineering Department Middle East Technical University Inönü Bulvari, 06531 Ankara, Turkey
3. Sheng W, Xi N, Song M, Chen Y (2001) CAD-guided robot motion planning. Industrial Robot: An International Journal Volume 28 Number 2 2001 pp. 143-151
4. Chen H, Xi N (2002) Automated robot trajectory planning for spray painting of free-form surfaces in automotive manufacturing. Proceedings of the 2002 IEEE International Conference on Robotics & Automation, Washington DC
5. Chen H, Xi N (2008) Automated tool trajectory planning of industrial robots for painting composite surfaces. International Journal of Advanced Manufacturing Technology (2008) 35: 680-696
6. Omar M, Viti V, Saito K, Liu J (2006) Self-adjusting robotic painting system. Industrial Robot 33/1(2006) 50-55
7. Atkar P, Greenfield A, Conner D, Choset H, Rizzi A (2005) Uniform coverage of automotive surface patches. The International Journal of Robotics Research 2005; 24; 883
8. Asakawa N, Takeuchi Y (1997) Teachingless spray-painting of sculptured surface by an industrial robot. Proceedings of the 1997 IEEE International Conference on Robotics and Automation, Albuquerque, New Mexico – April 1997
9. Anand S, Egbelu P (1994) On-line Robotic Spray Painting Using Machine Vision. International Journal of Industrial Engineering (1994) pp.87-95

10. Pichler A, Vincze M, Andersen H, Madsen O, Hausler K (2002) A method for automatic spray painting of unknown parts. Proceedings of the 2002 IEEE International Conference on Robotics & Automation, Washington DC
11. Asiabanpour B, Khoshnevis B (2004) Machine path generation for the SIS process. Robotics and Computer-Integrated Manufacturing 20 (2004) 167-175
12. Yao M, Xu B (2007) Evaluating wrinkles on laminated plastic sheets using 3D laser scanning. Measurement Science and Technology. pp. 3724-3730
13. Yang DO, Feng HY (2005) On the normal vector estimation for point cloud data from smooth surfaces. Computer-Aided Design 37 (2005) 1071-1079
14. Marchand (2003) Graphics and GUIs with MATLAB, 3rd edn. CRC Press, Boca Raton, FL
15. Tank (1991) Industrial paint finishing techniques and processes. Ellis Horwood, West Sussex, England
16. Talbert (2008) Paint technology handbook. CRC Press, Boca Raton, FL